The role of the cAMP/PKA and cGMP/PKG pathways in the regulation of the transbranchial ammonia excretion in the green shore crab, *Carcinus maenas*

by

Baoyue Zhang

A Thesis submitted to the Faculty of Graduate Studies of

The University of Manitoba

In partial fulfilment of the requirements of the degree of

MASTER OF SCIENCE

Department of Biological Sciences

University of Manitoba

Winnipeg

Abstract

As a toxic nitrogenous waste, ammonia causes ionoregulatory and neuronal dysfunction in aquatic animals. Without mechanisms to convert ammonia into less toxic molecules such as urea and uric acid, ammonotelic animals excrete ammonia directly into the surrounding environment. In order to deal with conditions causing possible elevated hemolymph ammonia levels, such as feeding, an efficient ammonia excretion process must be in place to keep the hemolymph ammonia levels within a tolerable range. While the excretory mechanisms of ammonia have been investigated in detail in fish and crustaceans, the intracellular regulation of these processes is basically unknown. To investigate the involvement of two key pathways, the cAMP/PKA and cGMP/PKG pathway, in the ammonia excretion process, gills from osmoregulating green shore crabs, *Carcinus maenas,* were isolated and perfused with hemolymph-like solutions containing either 200 µmol L^{-1} or 500 µmol L^{-1} NH_4Cl, mimicking the hemolymph ammonia levels in the resting state and after feeding, respectively. Basolateral application of the adenylyl cyclase activator or membrane-permeable 8-Bromo-cAMP, caused a significant decrease in the ammonia excretion rate. In addition, after PKA activation by 8-Bromo-cAMP, metabolically generated ammonia increased and the majority was now transported towards the hemolymph and not, as seen under control conditions, into the environment. Together, this suggests that the cAMP/PKA pathway promotes an ammonia retention mechanism. In contrast, activating the cGMP/PKG pathway by the application of membrane-permeable 8-Bromo-cGMP, resulted in an increase of the transbranchial ammonia excretion rate, which could be blocked by the PKG inhibitor KT5823. In addition, participation of nitric oxide synthase (NOS) in the cGMP synthesis *via* the soluble guanylyl cyclase is suggested due to the observed inhibitory effect on the branchial ammonia excretion after basolateral application of the NOS inhibitor L-NAME.

In conclusion, cGMP/PKG pathway, not the cAMP/PKA pathway promotes transbranchial ammonia excretion across the gill epithelium in *C. maenas*. The cAMP/PKA pathway is involved in a so far undescribed ammonia retention mechanism. The provided data will offer a basis for new venues investigating epithelial ammonia transport processes in general.

Acknowledgements

This research and dissertation are completed under the kind care and meticulous guidance of my supervisor Dr. Dirk Weihrauch. His serious attitude towards scientific research, rigorous spirit, and excellent work style have deeply inspired me. From the selection of the subject to the final completion of the project, he has always given me unremitting patience and support. Doing research is hard and sometimes confusing, but after each discussion with him, I feel more confident about myself and the path I have chosen. Here I would like to express my sincere gratitude and high respect to him.

I would also like to thank my committee members, Dr. Gary Anderson and Dr. Jason Treberg, for going above and beyond their duties and for their continuous guidance along the way.

Further, I would like to thank all members of the “Crab Lab”, who have spent a happy postgraduate life together. It is because of their help and support that I have been able to overcome difficulties and keep move forward. Special thanks to my friend Holly Whiting, in addition to supporting my academic work, she also invites me to family gatherings on every major holiday, sharing me culture and customs in the country and making me feel welcome here.

When the paper is about to be completed, my mood cannot be calm, from the beginning of the project to the completion of the paper, I have gained many helps and supports from teachers, classmates, friends and family, here please accept my sincere gratitude!

Table of contents

List of tables

List of figures

1. Introduction

1.1. Origin of ammonia

Ammonia, in here referring to both the gaseous form NH_3 and the ionic form NH_4^+, is a metabolic product of protein and nucleic acid metabolism. As consumers, aquatic crustaceans obtain nitrogen compounds, such as proteins and nucleic acids, from plants and animals they have consumed. The amino group removed from amino acids during the process of deamination is either re-used for the synthesis of new amino acids or released as ammonia into the body fluids after additional hydrogenation. In addition, for invertebrates it has been described that ammonia can also be generated as a side-product in the purine nucleotide cycle (Weihrauch et al., 2004b). With few exceptions, land-living animals excrete the majority of their nitrogenous waste either in form of uric acid (insects, birds, reptiles) or urea (mammals, adult amphibians) (Wright, 1995). In contrast to this, with the exceptions of elasmobranchs, Sarcopterygii (e.g. Coelacanths) and aquatic living mammals (e.g. Cetacea), aquatic living animals, such as teleost fish and basically all marine or freshwater dwelling invertebrates, are ammonotelic, excreting the majority (≥ 80%) of their nitrogenous waste directly as ammonia (Weihrauch et al., 2017).

1.2. Toxicity of ammonia

Ammonia is a highly toxic molecule. For instance, as an acid-base equivalent, ammonia can interrupt the cellular pH which is critical for enzyme functionality (Martinelle and Häggström, 1993). However, its main toxicity is based on its effects on the nervous system. Hydrated NH_4^+ and K^+ are very similar in size with an ionic radius of 1.45 Å and accordingly, it has been reported that ammonium affects the membrane potential of mammalian neurons and giant axons of cephalopods, influencing nerve excitability (Lazarenko et al., 2017). In mammals hyperammonemia, a state of elevated systemic ammonia levels, results in abnormal accumulation of glutamine in the astrocytes, which in turn increases the osmolality of the cytoplasm and leads to cell swelling and cell death, symptoms associated with Alzheimer Type

II astrocytosis (Adlimoghaddam et al., 2016b; Butterworth, 2002). In addition, ammonia can directly activate N-methyl-D-aspartate (NMDA)-type glutamate receptors in postsynaptic neurons, leading eventually to unregulated Ca^{2+} influx and cell death (Llansola et al., 2007). Due to its toxicity, ammonia concentrations in the body fluids must be kept within a tolerable range. Ammonotelic crustaceans are in general more tolerant towards elevated ammonia concentrations, when compared to mammals where circulating ammonia levels are usually low e.g. < 50 µmol L^{-1} in the serum of adult humans (Braissant et al., 2013) and < 70 µmol L^{-1} in the serum of mice after weaning (Koizumi et al., 1990). In decapod crabs, like the brackish water acclimated green shore crab *Carcinus maenas*, the seawater Dungeness crab *Metacarcinus magister*, or the freshwater acclimated Chinese mitten crab *Eriocheir sinensis*, the total hemolymph ammonia concentrations were measured between 100 and 200 µmol L^{-1} (Weihrauch and McGaw, 2023). Nonetheless, in a number of aquatic crustaceans, environmental ammonia is lethal in relatively low concentrations. In the Sao Paulo shrimp *Penaus paulensis*, LC_{50} after 96h exposure was determined to be 307 µmol L^{-1} total ammonia and in the red tail prawn *Penaus penicellatus* 1.39 mmol L^{-1} total ammonia (Weihrauch et al., 2017).

In addition, non-lethal high environmental ammonia (HEA) concentrations have been found to interrupt physiological processes such as ion regulation and immune function in crustaceans (Le Moullac and Haffner, 2000). Acute ammonia exposure (1.7 mmol L^{-1} for 48 h) in the mud crab *Scylla paramamosain*, induced oxidative stress and apoptosis (Cheng et al., 2019), while long-term HEA exposure resulted in heat shock response, DNA damaging and apoptosis in swimming crab *Portunus trituberculatus* (Lu et al., 2022). Moreover, after a 2-week chronic HEA exposure (1 mmol L^{-1}), a complete loss of active branchial ammonia excretion was observed in *M. magister* (Martin et al., 2011). In *C. maenas*, once the environmental ammonia concentration exceeds 1 mmol L^{-1}, an increase in branchial ion permeability was observed, disrupting the osmoregulatory capacity of the organism (Spaargaren, 1990).

1.3. Gills as the main site for ammonia excretion in aquatic crustaceans

In decapod crabs, ammonia is excreted through internal and external organs, namely the antennal gland, a kidney-like structure, and the phyllobranchiate gills, respectively (Fig. 1) (Freire et al., 2008). In the antennal gland of crabs, the primary urine is formed through ultrafiltration (Freire et al., 2008). In the final urine total ammonia concentrations vary between 70 µmol L^{-1} (*M. magister*) and almost 400 µmol L^{-1} (brackish water acclimated *C. maenas*). Nonetheless, the main site for ammonia excretion in decapod crabs are, as in many other aquatic dwelling organisms, the gills (Freire et al., 2008; Weihrauch and O'Donnell, 2017; Wright et al., 1995). In decapod crabs the gills are located in the well-ventilated branchial chambers. As multifunctional organs, the gills contribute, among other things, to gas exchange, osmoregulation, acid-base regulation, and ammonia excretion (Henry et al., 2012). With a stabilizing cuticle, gills of crustacean are excellent model tissues for investigating osmoregulatory NaCl transport and ammonia transport strategies using the preparation of the isolated perfused gill (Allen and Weihrauch, 2021; Henry et al., 2012).

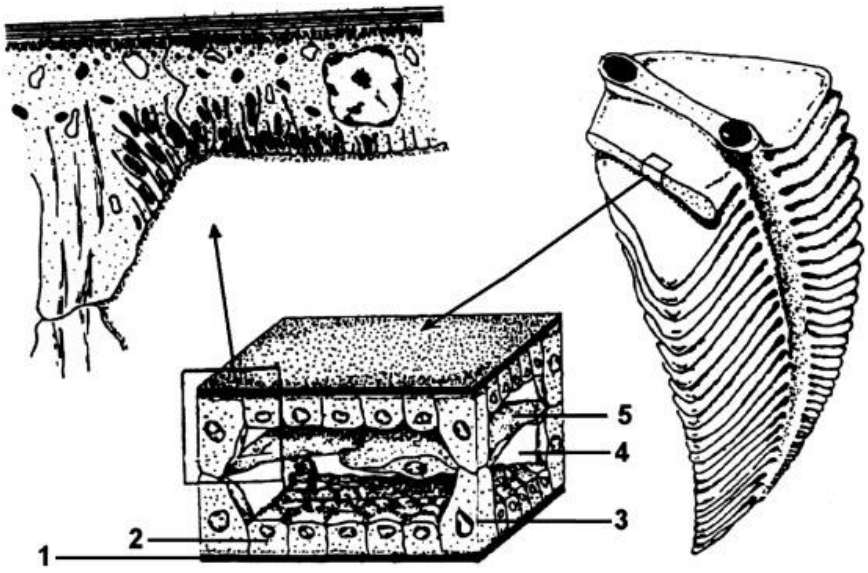

Figure 1. Schematic representation of morphology and fine structure in a transporting, posterior crab gill. 1, cuticle; 2, thick cell; 3, pilaster cell; 4, hemolymph space; 5, intralamellar septum (Freire et al., 2008).

In aquatic crabs, ammonia is excreted through the gills in both passive and active manners. The regular physiological pH in the hemolymph ranges from 7.7 to 8.0 (Meseck et al., 2016; Morris and Butler, 1996). Since ammonia is a weak base with a pKa of *ca.* 9.3 (Cameron and Heisler, 1983), the vast majority of ammonia exists here in the form of the ammonium ion, NH_4^+. The gaseous form of ammonia, NH_3, can diffuse to a certain degree across the cell membrane (Weihrauch et al., 1998), along the paracellular pathway, or *via* gas channels, e.g. the Rh-proteins (Quijada-Rodriguez et al., 2024), along an outwardly directed partial pressure gradient. Interestingly, for all decapod crabs investigated, NH_4^+ is excreted in an active mode over the gill epithelium, shown directly in gill perfusion experiments in *E. sinensis*, *M. magister*, and the edible crab *Cancer pagurus* (Weihrauch et al., 2004b).

For *C. maenas*, an euryhaline animal that thrives in brackish water and sea water, it has been shown that their gills are able to excrete actively against a 4-fold inwardly directed ammonia gradient (Weihrauch et al., 1998). Here the observed stark inhibition (*ca.* 80 %) of the branchial ammonia excretion after inhibition of the dynamic microtubule network (Weihrauch et al., 2002), strongly suggests that the vast majority of ammonia excretion is transported in an active energy consuming manner.

1.3.1. Ammonia excretion/transport mechanism across the gill epithelium of *C. maenas*

The green crab *C. maenas*, has been used as a model for exploring physiological processes for nearly a century. Isolated gills from brackish water acclimated *C. maenas* produce a measurable transmembrane potential difference (PD_{te}) due to an active branchial Cl^- uptake, driven solely by the basolateral localized Na^+/K^+-ATPase (Riestenpatt et al., 1996). As mentioned above, gills of this crab have been shown to promote an active ammonia excretion (Weihrauch et al., 1998). This active excretion mechanism depends on at least 3 energy consuming processes. 1) The Na^+/K^+-ATPase directly transports NH_4^+ from the hemolymph into the cytoplasm in exchange for Na^+ (Leone et al., 2017). In addition, the Na^+/K^+-ATPase creates a negative cell potential by excreting 3 Na^+ out of the cytoplasm and importing only 2 K^+. This negative cell potential is then driving cations, including NH_4^+, into the cytoplasm

either by NH_4^+ permeable K^+-channels (Cs^+-sensitive K^+ -channel (Weihrauch et al., 1998) and/or a hyperpolarization activated cyclic nucleotide-gated K^+-channel (HCN) (Fehsenfeld and Weihrauch, 2016)), or an amiloride-sensitive, likely electrogenic cation/Na^+ exchanger (Fehsenfeld and Weihrauch, 2015). The Na^+/K^+-ATPase likely also drives the Na^+ -dependent Hippocampus abundant transcript 1 (Hiat1), a recently discovered NH_4^+ transporter (Fehsenfeld et al., 2023b), and an apical localized NHE (Towle et al., 1997), which acidifies the subcuticular space, promoting apical ammonia trapping. Note, cellular localization of Hiat1 has not been confirmed yet. However, a morpholino knock-down in zebrafish larvae showed a reduced ammonia excretion in the ammonia excreting yolk sac and the pharyngeal region, which develops later into the gills (Zhouyao et al., 2022). 2) The second active component in branchial ammonia excretion is V-ATPase. Blocking this pump by bafilomycin A_1 caused a 66% inhibition of active branchial ammonia excretion. In *C. maenas*, this pump is localized on the membrane of cytoplasmatic vesicles in branchial epithelial cells (Weihrauch et al., 2001). It is proposed that the pump acidifies the lumen of vesicles generating a partial pressure gradient for NH_3. NH_3 diffuses along this gradient into the vesicles either *via* membrane diffusion or *via* a gas channel, potentially a Rhesus-like ammonia transporter, Rh2 (Genbank accession# AAK50057.2). Inside of the vesicles NH_3 is protonated to NH_4^+, which is then trapped inside of the vesicular lumen. 3) The third active component is the dynamic microtubule network. It is thought that NH_4^+-loaded vesicles are transported *via* the microtubule network to the apical membrane where NH_4^+ is released by exocytosis. This assumption was drawn from the fact that the active excretion process was nearly completely inhibited by colchicine, thiabendazole, and taxol (Weihrauch et al., 2002). In addition, NH_3 can diffuse *via* an apically localized Rh-protein (Rh1), a gas channel (Quijada-Rodriguez et al., 2024). The transport mechanism is summarized in a working model (Fig. 2).

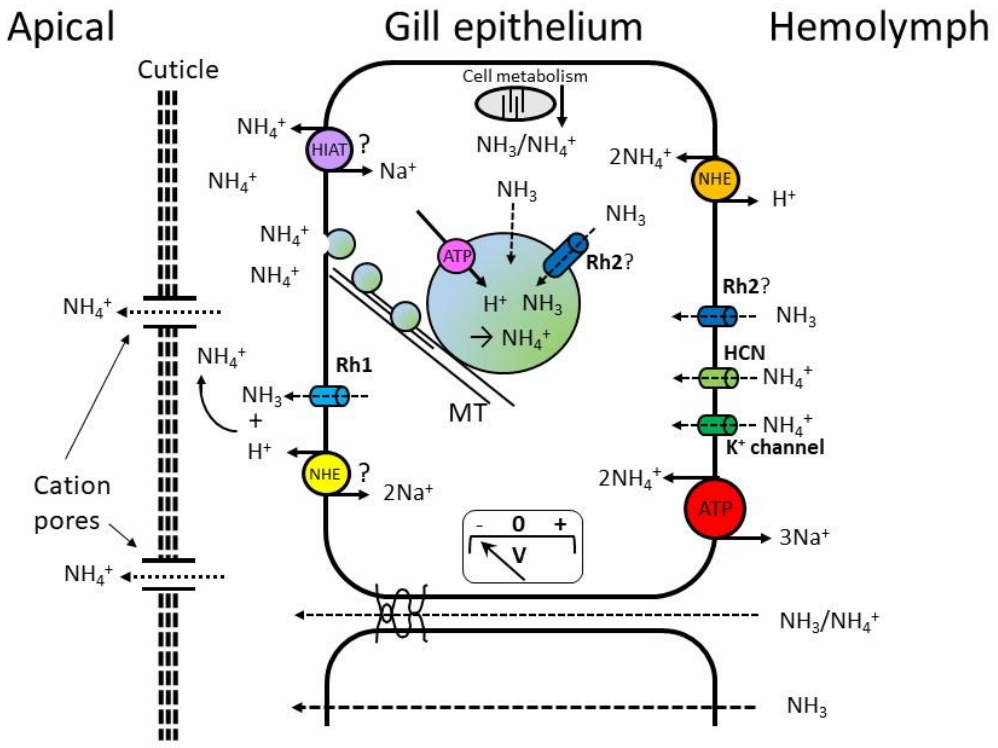

Figure 2. Proposed working model for the mechanism of ammonia transport across the gill epithelium of *C. maenas*. For explanation refer to the text under 1.3.1. Note, ammonium pores in the cuticle were suggested due to the observation of a dose-dependent inhibition of the ammonia flux over the isolated cuticle using amiloride (Weihrauch et al., 2002). ? indicates: a) suggested presence of a second Rh-protein (Rh2) in the basolateral and/or vesicular membrane (Genbank accession# AAK50057.2); b) an apical localized NHE (Towle et al., 1997) that may acidifies the subapical space; c) unknown localization of an identifies Na^+-dependent NH_4^+ transporter, Hiat1 (Fehsenfeld et al., 2023b).

1.3.2. The role of the Na^+/K^+-ATPase in branchial osmoregulation and ammonia excretion

As one of the most important ion pumps in epithelial cells in the crustacean gills, Na^+/K^+-ATPase is involved in both branchial osmoregulatory NaCl uptake and branchial ammonia excretion (Halperin et al., 2004; Weihrauch et al., 2002). With the exception of freshwater dwelling crustaceans where the V-ATPase also plays a significant role in branchial NaCl uptake (Weihrauch et al., 2004a), the Na^+/K^+-ATPase is the key transporter responsible for active NaCl uptake in the gills of hyper-regulating crabs. This was supported by enzyme activity assays and gene expression studies in gills of crabs acclimated to various salinities (Towle et al., 2011), electrophysiological studies (Onken and Siebers, 1992), and tracer flux studies (Riestenpatt et

al., 1996), employing the Na^+/K^+-ATPase - specific inhibitor, ouabain (g-strophanthin). Interestingly, the Na^+/K^+-ATPase is also directly involved in transepithelial ammonia transport as described above for branchial ammonia excretion in *C. maenas* or *M. magister* (Allen et al., 2024), but also for other aquatic species such as the gills of fish (Weihrauch et al., 2009), the cutaneous excretion in planarians and leeches (Weihrauch et al., 2012), the excretory mechanism in the anal papillae of mosquito larvae (Durant and Donini, 2019), and the ammonia excretion mechanism in the mammalian large intestine (Worrell et al., 2008).

In fact, it has been shown in amphibians (Cruz et al., 2013), fish (Sinha et al., 2013), freshwater leeches (Quijada-Rodriguez et al., 2017), roundworms (Adlimoghaddam et al., 2016a), and Horseshoe crabs (Hans et al., 2018), that the Na^+/K^+-ATPase accepts NH_4^+ as a substrate in place of K^+. For some crustaceans, e.g. *Callinectes danae* and the freshwater prawn *Marcobrachium olfensii*, it has been demonstrated that NH_4^+ can synergistically stimulate the Na^+/K^+-ATPase in enzyme assays which were analyzed under conditions optimized for activity measurements (Leone et al., 2017).

It needs to be mentioned that, in contrast to suggested mechanisms in fish (Wright and Wood, 2012), the NaCl uptake and ammonia excretion mechanism in invertebrates - although mediated in the same tissue and with common participation of the Na^+/K^+-ATPase - functions independent of each other. For instance, while the active branchial ammonia excretion in *C. maenas* was massively inhibited by blocking the V-ATPase (*ca.* 66%) or the functional microtubules network (90-100%), no inhibitory effect was observed for the NaCl uptake employing these inhibitors (Weihrauch et al., 2002).

While ammonia transport/excretion pathways have been studied extensively in mammals (kidney), fish and numerous invertebrates, including roundworms, planarians, leeches, insect larvae and crustaceans (Weihrauch and Allen, 2018), cellular pathways regulating epithelial ammonia transports have not been investigated in depth neither in vertebrate nor invertebrate systems.

1.4. The cAMP/PKA and cGMP/PKG pathway

As “second messengers”, both cyclic adenosine monophosphate (cAMP) and cyclic guanosine monophosphate (cGMP) transduce signals from extracellular stimulation into intracellular activation cascades.

1.4.1. Cyclic AMP and protein kinase A (PKA)

Cyclic AMP is produced by a membrane-bound and/or by a cytoplasmic soluble adenylyl cyclase (AC), catalyzing ATP into cAMP and inorganic pyrophosphate (Rahman et al., 2013; Schuster et al., 2024) (Fig. 3). While the activity of soluble AC could be regulated by the presence of HCO_3^- and Ca^{2+} (Litvin et al., 2003), the activity of membrane-bound AC is often regulated by the activation of G protein-coupled receptors (GPCRs) (Ostrom et al., 2022). As the sensor of extracellular signals, GPCRs at the cell surface experience conformational change after the interaction with extracellular stimulators, activating associated G proteins. When guanosine diphosphate is released from the α-subunit of the G protein, the trimeric G protein dissociates into an α-subunit and a βγ-heterodimer which can either activate or inhibit the activity of the membrane-bound AC (Schuster et al., 2024). There are many target effector proteins of cAMP, including protein kinase A (PKA) (Taylor et al., 2013) (Fig. 3), nucleotide-gated ion channels (Napolitano et al., 2021), and exchange proteins (Purves et al., 2009; Robichaux and Cheng, 2018). This action then regulates a series of cellular processes, such as ion transport (Ni et al., 2006), exocytosis (Seino and Shibasaki, 2005), and cell adhesion (Vielmuth et al., 2023). In eukaryotic cells, the function of cAMP mainly relies on protein kinase A (PKA), which is in general activated *via* an increase of cAMP concentrations (Cheng et al., 1998). Normally, in auto-inhibition format, the heterotetrametric PKA has two catalytic subunits and two regulatory subunits, with two cAMP binding domains in each regulatory subunit. Binding of cAMP to the regulatory subunits of PKA causes a dissociation between the regulatory and catalytic subunits, unmasking the catalytic subunits to phosphorylate target proteins (Francis et al., 2002). As a well-studied enzyme in the cAMP cascade, PKA has been

shown to play roles in many biological processes. Among other things, PKA activates the Na^+/K^+-ATPase by phosphorylation of Ser-943 on the alpha subunit (Poulsen et al., 2010), driving key transporter-related mechanisms in the cell. In addition to the Na^+/K^+-ATPase, PKA has also been shown to activate the V-ATPase. Here it was demonstrated that PKA phosphorylates the subunit A of the cytosolic V_1 complex at Ser-175 in both *in vitro* and *in vivo* experiments (Alzamora et al., 2010). The V_1 complex is known to play a key role in regulating the localization and activity of V-ATPase (Alzamora et al., 2010). Moreover, Voss and coworkers showed that in the midgut of the lepidopteran tobacco hornworm *Manduca sexta*, PKA phosphorylates the C subunit (V_1 complex) of the V-ATPase regulating the reassembling of the holoenzyme (Voss et al., 2007).

Of note, PKA is a highly conserved kinase within the animal kingdom. For instance, the catalytic subunit 1 from the decapod American lobster *Homarus americanus*, (GenBank accession#: XP_042222749) displays 85% identity in the amino acid sequence to its mammalian counterpart (e.g. *Mus musculus,* GenBank accession#: NP_001264827).

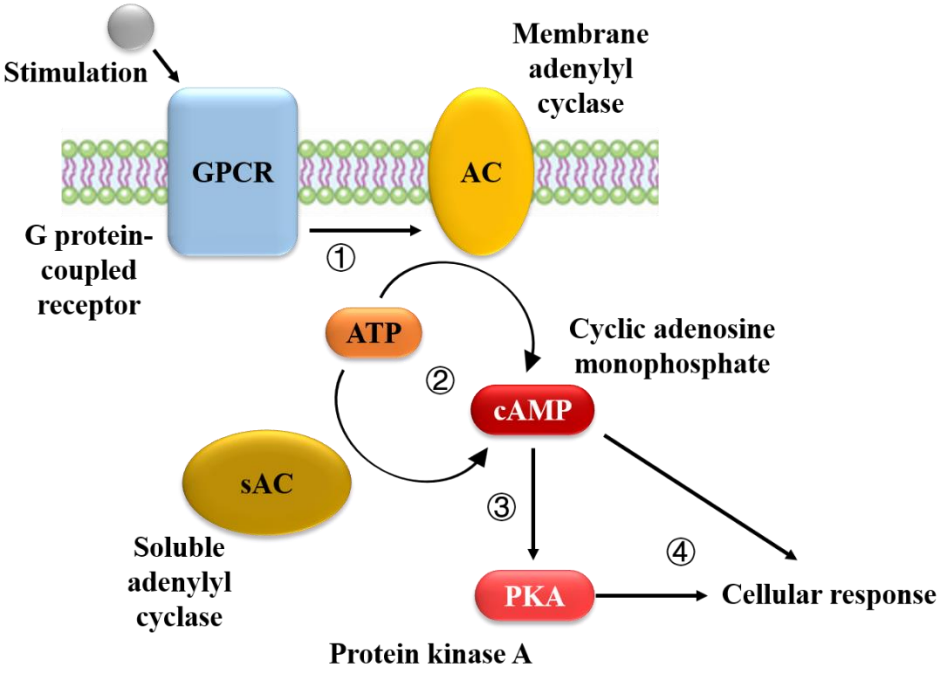

Figure 3. Simplified illustration of the cAMP/PKA pathway. 1, The activation of G protein-coupled receptors regulates the activation of the membrane adenylyl cyclase (Ostrom et al., 2022); 2, Both the membrane-bound and soluble adenylyl cyclase convert ATP into cAMP by removing a pyrophosphate molecule (Schuster et al., 2024); 3, PKA is activated by the binding of cAMP on the regulatory subunits, leading to conformational changes and dissociation of the catalytic subunits (Francis et al., 2002); 4, Both cAMP and PKA can regulate cellular

responses.

1.4.2. Cyclic GMP, protein kinase G (PKG), and nitric oxide synthase

Also, cGMP is a secondary messenger and is generated by the guanylyl cyclase (GC) from guanosine triphosphate (GTP). As lyase enzymes both the membrane-bound GC (pGC) and the cytoplasmic soluble GC (sGC) catalyze and convert GTP into cGMP and pyrophosphate (Pasmanter et al., 2019) (Fig. 4). While pGC is activated through neuroendocrine peptide hormones binding to its extracellular domain (Kobiałka and Gorczyca, 2000), the sGC is often activated by binding of nitric oxide (NO) (Derbyshire and Marletta, 2009; Pietrobon et al., 2011) (Fig. 4). Nitric oxide, as an intra- and intercellular messenger, can influence a variety of intracellular pathways. For example, in skeletal muscles of *Idotea baltica*, NO stimulated increase of cGMP production resulted in an increase of potassium currents (Hermann and Erxleben, 2001). Synthesized by NO synthase (NOS), gaseous NO often acts in a paracrine manner through diffusion from adjacent cells (Förstermann and Sessa, 2012). Using L-arginine as a substrate, NOS works as a homodimer, hydroxylating L-arginine into N^{ω}-hydroxy-L-arginine (L-NOARG), and then oxidizing it into L-citrulline and NO (Stuehr et al., 2001). In addition, rising intracellular Ca^{2+} levels could also indirectly contribute to the activation of GC by promoting the formation of NO *via* NOS (Pietrobon et al., 2011).

Cyclic GMP mediates its effects mainly through the regulation of ion channels (Bauer, 2002), interaction with phosphodiesterases (PDEs) (Rybalkin et al., 2003), and the activation of cGMP-dependent protein kinase (PKG) (Francis et al., 2010). As one of the primary direct effectors of cGMP, PKG exists as a homodimer with two identical subunits, containing an N-terminal domain (auto-inhibition kinase activity), a C-terminal catalytic domain, and a regulatory domain with two non-identical cGMP-binding sites (Wall et al., 2003). The activation of PKG depends on the binding of cGMP, inducing a conformational change to remove the inhibition of the N-terminal domain, making the catalytic site accessible (Wall et al., 2003). PKG regulates the activity, function and subcellular localization of target proteins *via* phosphorylation, transferring the phosphate from ATP to the hydroxyl group of a serine/threonine side chain of the target proteins (Francis et al., 2010). PKG plays key roles in many physiological processes, including promoting neural cell survival (Francis et al., 2002),

maintaining vascular homoeostasis (Burgoyne et al., 2012), and preventing the aggregation of platelet cells (Gambaryan, 2022). In CA1 pyramidal cells of rats, PKG inhibits the activity of the Na^+/K^+-ATPase, inducing a suppression of Na^+/K^+-ATPase-generated after-hyperpolarization (Mohan et al., 2019). In addition, the NO/cGMP/PKG pathway has been shown to regulate the relaxation of smooth muscles through decreasing concentrations of intracellular Ca^{2+} (Lincoln, 1983).

Also, PKG and NOS are considered being conserved within the animal kingdom. For example, the amino acid sequence of the mammalian cGMP-dependent protein kinase 1 (isoform beta from *Mus musculus*, Genbank accession # NP_035290.1) and the cGMP-dependent protein kinase, isozyme 1 in the gazami crab *Portunus trituberculatus* (Genbank accession # MPC59629.1) exhibit 68% identity. In addition, the amino acid sequence of NOS in *C. maenas* (Genbank accession # ACY56317.1) shares 76% identity with NOS of *Rattus norvegicus* (GenBank accession#: AAC02242.1).

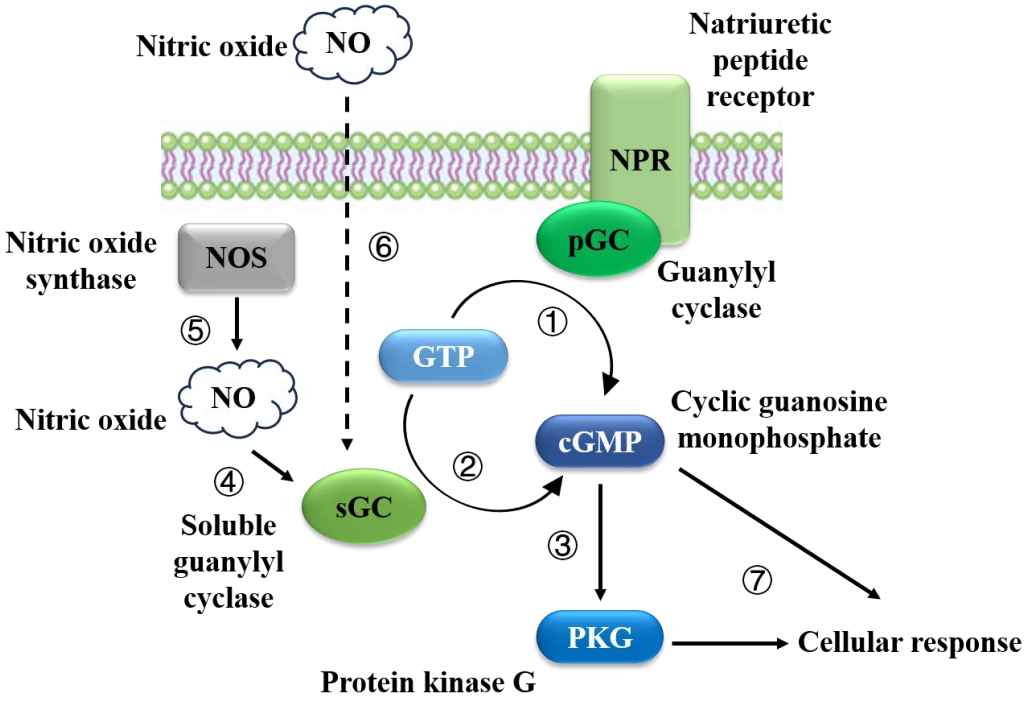

Figure 4. Simplified illustration of the cGMP/PKG pathway. cGMP is produced by either the membrane-bound guanylyl cyclase (1) or the soluble guanylyl cyclase (2) by removing pyrophosphate from GTP; 3, cGMP activates PKG by removing a pseudosubstrate domain that frees the catalytic site. The activity level of PKG is directly proportional to the cGMP concentration (Pasmanter et al., 2019); 4, NO activates sGC by binding to the heme cofactor of the enzyme and causing a conformational change; the source of NO is from either the production

of NO synthase (5) or gas diffusion (6) from hemolymph or adjacent cells (Förstermann and Sessa, 2012). 7, Both cGMP and PKG can regulate cellular responses.

1.5. Objectives and hypothesis

1.5.1. Objective

The objective of this study is to investigate the so far unknown roles of the PKA and PKG signaling pathways in branchial ammonia excretion of *C. maenas*. For this, the presence of the branchial membrane-bound and soluble guanylyl cyclase, and the nitric oxide synthase will be confirmed by endpoint PCR. Participation in branchial ammonia excretion of cAMP, cGMP, nitric oxide synthase (NOS), PKA, and PKG will be investigated by employing the preparation of the isolated perfused gill and specific activators or inhibitors for the enzymes and the use of membrane-permeable proxies for cAMP and cGMP, 8-Bromo-cAMP and 8-Bromo-cGMP, respectively.

1.5.2. Hypothesis

Hypothesis 1

A study on the hyperregulating rainbow crab *Chasmagnathus granulatus* showed by measuring the transepithelial potential difference (PD_{te}) that both forskolin and cAMP stimulate transbranchial NaCl uptake. Additionally, it was demonstrated that forskolin led to an increase of Na^+/K^+-ATPase activity of the crab (Halperin et al., 2004). Moreover, Dames and coworkers strongly suggested that cAMP mediates the reversible assembly and activation of V-ATPase in salivary glands in insects (Dames et al., 2006). Since both, the Na^+/K^+-ATPase and the V-ATPase are directly involved in active ammonia excretion in the gills of *C. maenas*, it is hypothesized that the cAMP/PKA pathway actives the transbranchial ammonia excretion mechanism in this crab.

Hypothesis 2

Using the perfused gill preparation, Fehsenfeld and co-workers showed that the crustacean hyperglycemic hormone (CHH) caused a significant increase in branchial ammonia excretion in *C. maenas* (Fehsenfeld et al., 2023a). In addition, knock-down studies in the white shrimp *Litopenaeus vannamei*, by Zhang and co-workers suggested that CHH also promotes ammonia excretion *via* Rh-proteins and exocytosis (Zhang et al., 2020). Earlier Chung and Webster demonstrated that application of CHH causes a more than 10-fold increase in cGMP levels in gills and the hindgut of *C. maenas* (Chung and Webster, 2006). It is therefore hypothesized that the cGMP/PKG signaling pathway is involved in branchial ammonia excretion in *C. maenas*, potentially also activating this process.

2. Methods and materials

2.1. Animals

Adult male green shore crabs *C. maenas* (carapace width 5 - 7 cm), were collected from the Northern Placentia Bay (NF, Canada) and transported on ice to Winnipeg (MB, Canada) to be housed at the Animal Holding Facility (University of Manitoba, Winnipeg, Manitoba, Canada). Here animals were kept in 300-gallon tanks containing recirculating artificial sea water (SW) (Fritz Reef Pro Mix (RPM), USA). The SW was adjusted to a salinity of 32 ppt, a pH of 8.0 and a temperature of 16°C. The SW was oxygenated by multiple air stones. Animals were kept under a light:dark cycle of 12:12 hours. Shrimp meat was supplied twice a week as a food source, and un-eaten remaining food was removed one day after feeding to prevent any contaminations from putrefaction.

Before the experiments, crabs were acclimated for at least two weeks to diluted artificial seawater (brackish water, BW; 10 ppt; pH 7.9-8.0, 16°C). For each SW to BW transition process, 8-10 crabs were first transferred into a 20-30 L tank of aerated SW and salinity was reduced slowly over a time period of 2 hours till a target salinity of 10 ppt was reached. Then crabs were transferred into a 300-gallon BW tank for further acclimation. The BW tank contained no more than 20 individuals at any time to avoid any pH drop or enrichment of ammonia.

The pH and KH (carbonate hardness) of the tank water was monitored every two days for pH (accumet®, Fisher, US) and KH (API®, Mars Fishcare, US) respectively. Reef Buffer™ (Seachem® Laboratories, ID39022, USA) was added into the tank when needed to adjust the pH to 8.0. Reef Builder™ (Seachem® Laboratories, USA) was used to maintain the KH at around 6. Continuous air supply was provided by air stones. PVC pipe was provided as shelters.

Crabs used for gill perfusion were starved for at least 2 days before each experiment to avoid the effects of elevated hemolymph ammonia levels after feeding (Quijada-Rodriguez et al., 2022).

2.2. Measurement of branchial ammonia transport using the preparation of the isolated posterior gill

Osmoregulatory active posterior gills (gills 7, 8, and 9) from *C. maenas* (Fig. 5 A) were isolated and used for gill perfusion experiments according to previous protocols and techniques (Siebers et al., 1985). Crabs were anaesthetized on ice for at least 20 minutes before removal of the carapace. Posterior gills were excised by scissors, and then transferred into a petri dish containing the bathing solution (composition in mmol L^{-1}: 260 NaCl, 8 KCl, 7 $MgCl_2$, 7 $NaHCO_3$, 5 $CaCl_2$, adjusted with 2.5 Tris to a pH of 7.8). The ion concentrations in the bathing solution were kept similar in composition to the perfusion solution and close to solutions employed in previous studies on branchial ammonia excretion and osmoregulatory NaCl uptake in *C. maenas* (Onken and Riestenpatt, 2002; Postel et al., 1998; Weihrauch et al., 1999; Weihrauch et al., 1998; Weihrauch et al., 2002).

The perfusion solution was delivered by a fine plastic polyethylene tube ($ø_I$ 1.14 mm, $ø_O$ 1.57 mm, IntraMedic™) inserted into the afferent vessel of the gill. The tube was attached to a soft manifold pump tube ($ø_I$ 0.76mm, IW019767, Fisher scientific, USA) linking to a peristaltic pump (WATSON-MARLOW 323, England) (Fig. 5 B). The perfusion rate was set to 130-150 µL per minute. In order to avoid air bubbles entering the gill vessel, home-made dripping joints/air traps were used at every connection point.

For the collection of the perfusate, another fine tube was inserted now into the efferent vessel of the gill and the open end of the tube was place into a pre-weighted collection beaker. Home-made gill clamps and cotton thread were used to secured the position of the tubes within the gills and to prevent leakage. Gills were placed in a beaker containing 25 mL of the bathing solution (Fig. 5 C).

If not mentioned otherwise, each perfusion experiment consisted of 3 collection periods of 30 min. a) a control stage to define the basal ammonia transport rate by the individual gill; b) an experimental stage in which respective activators and inhibitors were applied; c) a wash-out step in which the integrity/decay of the gill tissue is monitored. Prior to each stage there was a 15-minute wash-in/wash-out period (no sampling).

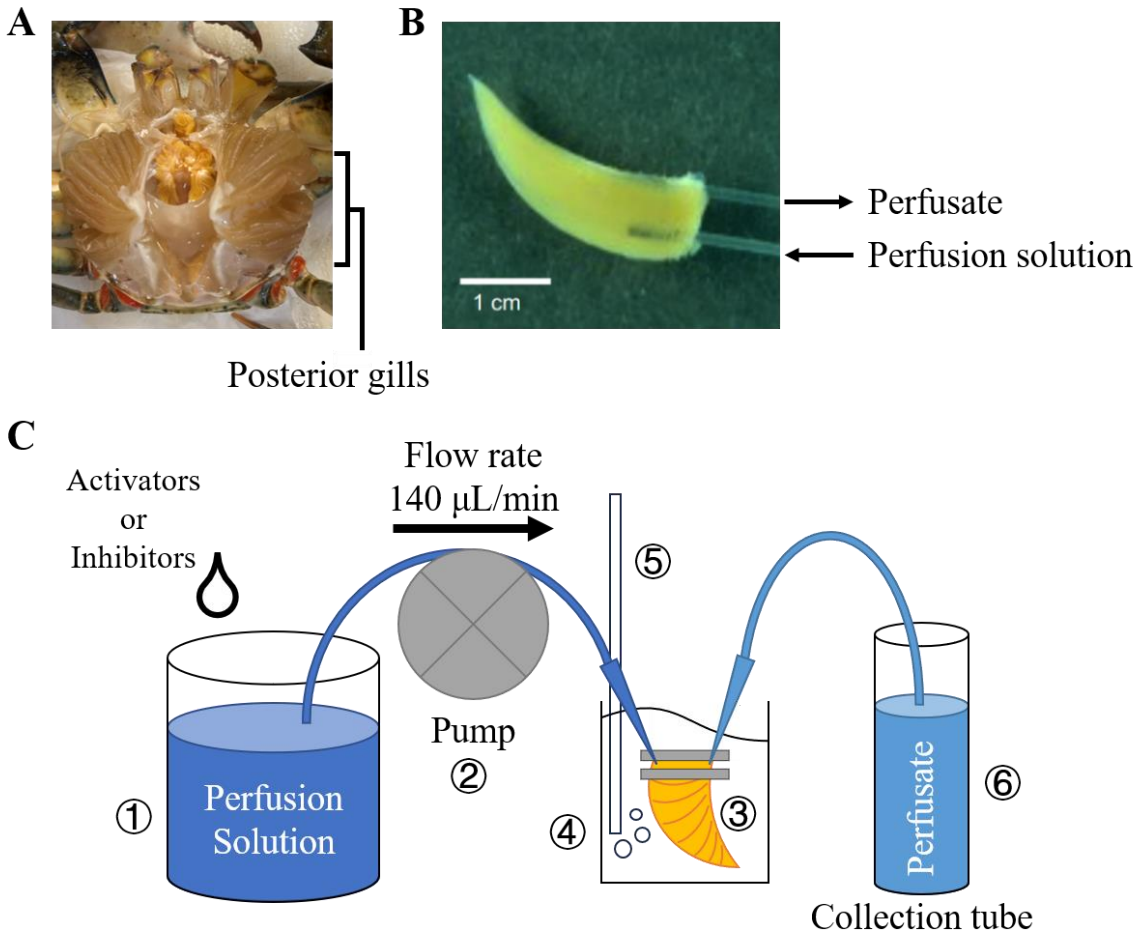

Figure 5. Animals, materials and gill perfusion set-up. A) Green shore crab, *C. maenas*, carapace was removed, showing posterior gills used for isolation. B) Isolated perfused gill. The afferent vessel is linked to the pump; the efferent vessel is linked to the collection tube (Weihrauch and Allen, 2018) C) Set-up for perfusion experiment. 1, perfusion solution, serving hemolymph-like solution containing either 200 or 500 µmol L^{-1} NH_4Cl, with or without additional activators and inhibitors; 2, pump is transporting hemolymph-like solution by means of tubes into the afferent vessel of the gill; 3 isolated gills, the top of the gill is clamed and tied up to secure the position of tubes; 4, bathing solution, submerging the isolated gill completely; 5, air supply; 6, collected perfusate, solution after one gill passage is collected.

The hemolymph-like perfusion solution consisted of (in mmol L^{-1}): 260 NaCl, 8 KCl, 7 $MgCl_2$, 7 $NaHCO_3$, 5 $CaCl_2$, 0.5 Glutamine, 0.3 Glucose and 0.1 Glutathione, adjusted with 2.5 Tris to a pH of 7.8 according to previous studies (Fehsenfeld and Weihrauch, 2013). Depending on the experiment, the perfusion solution was enriched with 0.2 mmol L^{-1} NH_4Cl referring to steady state conditions (2 days after feeding hemolymph levels), or 0.5 mmol L^{-1}

NH_4Cl to mimic elevated ammonia levels observed after feeding (Quijada-Rodriguez et al., 2022). In experiments for measuring ammonia produced by gill metabolism, gills were perfused and bathed in solutions containing no ammonia at the beginning of each experimental step. Here each step lasted for 1 hour.

Notably, in the perfusion experiment to investigate the participation of NOS, an additional 30 minutes of perfusion with 1 mmol L^{-1} L-NG-nitroarginine methyl ester (L-NAME) was added into the sequence with a 30 min. pre-adaption period allowing the gills to use up endogenous cGMP/PKG before the application of 8-Bromo-cGMP. After each collection period the collection beaker was measured for the increase of weight (= volume of perfusate) on a fine balance. The collected perfusate was then transferred into a 15 mL Falcon tube. All collected samples were immediately stored at -20°C but not longer than 2 days before ammonia concentration measurement commenced (see 2.3.).

The time-dependent natural decay of the gill tissue during perfusion protocol has been tested in previous studies, showing a 16.3% decrease per hour of metabolic ammonia production (Weihrauch, 1995). For the current study the natural decay of gills' activity resulted in a 6% decrease per hour of the ammonia excretion rate (µmol Fwg^{-1} h^{-1}) when an 500 : 0 µmol L^{-1} NH_4Cl outwardly directed gradient was applied for 3 hours (tested in 6 gills from 5 crabs).

Activators and inhibitors were applied on the basolateral side of the gill by addition to the perfusion solution based on previous studies: Forskolin (adenylyl cyclase activator, Sigma, 93049, US) 10 µmol L^{-1} (Genovese et al., 2006); 8-Bromo-cAMP (cell-permeable cAMP analog, APEBIO, B9000) 10 µmol L^{-1} (Halperin et al., 2004); SQ22536 (adenylyl cyclase inhibitor, Millipore Sigma, 568500, China) 10 µmol L^{-1} (Xu et al., 2022); KT5720 (PKA inhibitor, MilliporeSigma, 420320, Israel) 250 nmol L^{-1} (Halperin et al., 2004); 8-Bromo-cGMP (MilliporeSigma, 203820, Germany) 5 µmol L^{-1}; KT5823 ($C_{29}H_{25}N_3O_5$, PKG inhibitor, Abcam, ab120423, US) 500 nmol L^{-1}; L-NG-nitroarginine methyl ester (NO synthase inhibitor, Sigma, N5751, US) 1 mmol L^{-1} (Pitts and Mykles, 2015).

At the end of each perfusion experiment, tubes were removed from the vessels and the gills were cut above the clamps. Cut gills were then placed between two sheets of soft paper

(KIMTECH®, Kimberly-Clark, US), and blotted dry under light pressure before weight determination using an electronic scale to determine the gills' fresh weight as conducted in previous experiments (Weihrauch et al., 1998).

2.3. Analysis of ammonia concentration

Samples were diluted with ammonia-free hemolymph-like perfusion solution before measurement to fit into the ideal, most sensitive range of ammonia concentration of the electrode (5 - 100 μmol L^{-1}).

The ammonia concentration in each sample was determined using an Orion™ NH_3 sensitive electrode (Thermo Electron Corporation, Beverly, Massachusetts, United States of America) connected to a digital pH meter (Beckman Coulter Corporation, Fullerton, CA, United States of America). This was accomplished by adjusting the pH of the sample to above 12 by adding 30 μL of 1 mol L^{-1} NaOH solution. This pH shift is required to convert all NH_4^+ to NH_3 (pKa = 9.3) which is the only form of ammonia the gas-selective probe can measure. During measurement, the sample was magnetically stirred at a constant rate (300 rpm) at room temperature by means of a magnetic micro stirring bar and probe measurements were taken when the mV reading was constant. Also, since probe values are reported in millivolts (mV), standard curves were generated by plotting mV readings (y-axis) against log-transformed concentration values (x-axis). Standard curves were also prepared in the expected concentration range using either dilutions of the employed respective perfusion solution or, in case to the measurements of the release of metabolic ammonia, the respective employed solutions were enriched with 5, 10, 20, 30, 40, or 50 μmol L^{-1} of NH_4Cl. For all standard curves an $R^2 \geq 0.98$ was required.

In addition, in previous studies, a slight drift in electrode readings was observed over time. This was compensated for by preparation of a calibration curve prior to and following measurement of each set of samples. Also, a sample of known ammonia concentration was analyzed periodically during analysis of each sample set in order to determine any drift of the electrode.

For the determination of net-fluxes, only the perfusion solution was considered, as the

majority of metabolically produced ammonia is release (under control conditions) towards the apical bath (Weihrauch et al., 1998). By this the calculated net efflux is at best underestimated.

Net fluxes were expressed in µmol Fw g^{-1} h^{-1} and calculated according to:

Net excretion rate = [($C_{initial}$ - $C_{perfusate}$) * volume collected] / [collection time * fresh weight].

Here $C_{initial}$ reflects the ammonia concentration (µmol L^{-1}) of the initial perfusion solution and $C_{perfusate}$ reflects the ammonia concentration (µmol L^{-1}) of the perfusate after one passage through the gill.

In the experiments for detecting metabolic ammonia of the gill tissue itself, both the perfusate and the bathing solution were analyzed for their ammonia content after each collection stage.

2.4. Determination of mRNA presence of NO-synthase, pGC and NO-sensitive sGC in the branchial tissue of *C. maenas*

Crabs acclimated to 10 ppt were placed on ice for 20-30 minutes and the posterior gill 9 was dissected under RNase-free conditions. RNA was extracted using TRIzol® (Thermo Scientific, US) according to the manufacture instruction. The quantity and quality of the extracted RNA was then determined spectrophotometrically by the NanoDrop™ (Thermo Scientific, US). RNA integrity was checked by loading the isolated RNA (*ca.* 0.5 µg) on a 1.3 % agarose gel to observe sharp ribosomal bands and no smear which would indicate degradation. Before being reverse transcribed into cDNA using LunaScript® RT SuperMix Kit (New England Biolabs, Ontario, Canada), DNase I (Thermo Scientific, US) was applied to remove remaining genomic DNA contamination in the RNA samples. Complementary DNA was synthesized from 0.5 µg RNA using BioRad iScript™ cDNA Synthesis Kit (BioRad, US). The quality of cDNA was checked by an application of primers for arginine kinase (Table 1) as positive control.

The nucleotide sequences for NO-synthase (NOS; GBXE01134821.1), membrane guanylate cyclase (pGC; GFXF01288729.1) (Oliphant et al., 2018), and NO-sensitive soluble guanylate cyclase (sGC1b; AGB51123.1) were obtained from pervious study (Abuhagr et al.,

2014). Primers for NOS, pGC and sGC1b were generated through Primer3 (Table 1). PCR reactions were performed employing Econo Taq® Green Plus Supermix (Biosearch Technologies, Hoddesdon, UK) and 2 µL of cDNA. PCR products were separated on a 1.3% agarose gel containing ethidium bromide and TAE buffer. Gel fragments were purified using the GeneJET Gel extraction kit (Thermo Scientific, US), re-amplified and sent off for sequencing at The Centre for Applied Genomics (Toronto, ON, CA). The resulting sequences were blasted against the NCBI database to ensure the correct amplicon.

Table 1. Primer sequences employed in endpoint PCR for the posterior gills of *Carcinus maenas*.

Transcript	GenBank accession no.	Forward primer sequence (5' → 3')	Reverse primer sequence (5' → 3')	Amplicon size (bp)	Annealing T [℃]
NO synthase (NOS)	GBXE01134821.1	AGTTGGAGCTGCAGTGGTAT	ACCAATCTCGGACACCATGT	116	59
Membrane guanylyl cyclase (mGC)	GFXF01288729.1	CGTGTGTGCCTTTATCGGAG	TCATCCTCCGCCAGTATGTC	102	59
Soluble guanylyl cyclase beta 1 (cGC1b)	AGB51123.1	CAAGATGATGGGTTCGCCTT	CTCTCTGGTCGTGTCTCTGC	147	56
Arginine kinase (ArgK)	AF167313.1	CGCTGAGTCTAAGAAGGGATT	CCCAGGCTAGTCTTCTTGGCC	200	59, 56

2.5. Statistical analysis

Data derived from individual gills of a single crab were pooled and averaged (n = 1). The replicates of animals were considered as the N value of each experiment set. Statistical analyses were conducted using GraphPad Prism 5 (Boston, MA, USA). For comparing the changes of ammonia excretion rate among experimental steps, a one-way Anova repeated measures test was used with treatment as the independent variable. For all data sets, a *p* value lower than 0.05 was considered as significant different. Since data were generated by repetitive measurements on the same gill, *p* values are also provided using a paired t-test analysis comparing control values to the actual experimental step, if the *p* value of one-way Anova analysis was lower than 0.05 among all data without showing significant difference between any two perfusion steps. All data are presented as means ± SEM.

3. Results

3.1. Basic branchial ammonia excretion in the posterior gills of *C. maenas*

Before investigating any regulation of branchial ammonia excretion, the transbranchial ammonia excretion rate over the isolated perfused gill must be detected under the employed experimental conditions.

During one gill passage, the ammonia concentration in the initial perfusion solution was reduced from 200 µmol L^{-1} to 159.6 ± 5.7 µmol L^{-1} and from 500 µmol L^{-1} to 352.9 ± 10.6 µmol L^{-1}, respectively (Fig. 6 A). Further, when a 500 : 0 µmol L^{-1} ammonia gradient was applied, posterior gills from *C. maenas* excreted *ca.* 3 times as much ammonia (50.6 ± 3.0 µmol Fwg^{-1} h^{-1}) as when compared to the excretion rates measured under a 200 : 0 µmol L^{-1} ammonia gradient (16.9 ± 1.8 µmol Fwg^{-1} h^{-1}) (Fig. 6 B).

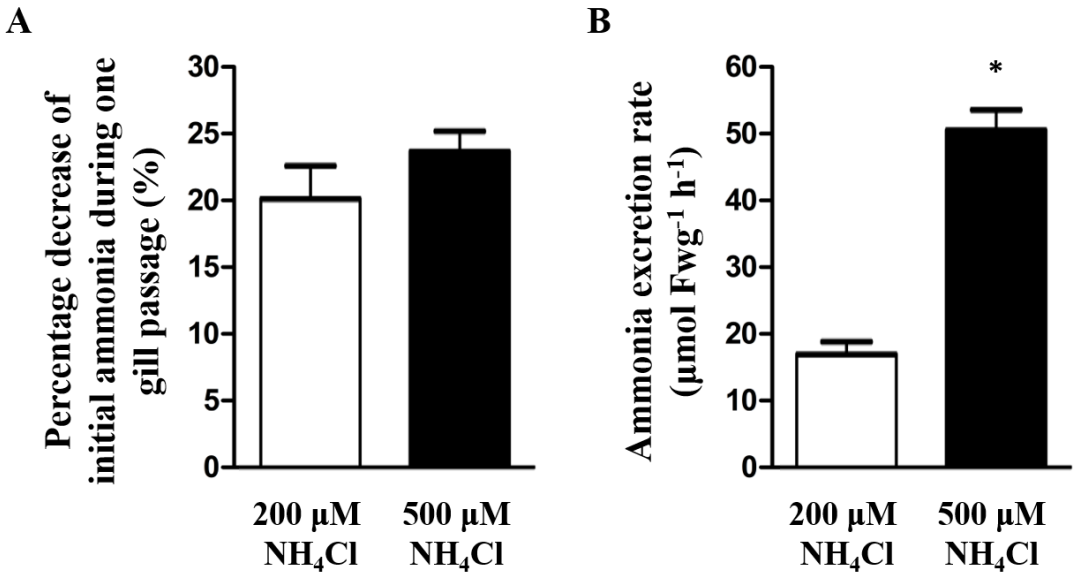

Figure 6. Basic branchial ammonia excretion in the isolated posterior gills of *C. maenas*. Gills were perfused with either 200 or 500 µmol L^{-1} ammonia while bathed in a solution that contained no ammonia at the beginning of the experiment. A) Percentage of ammonia loss from the perfusion solution during one single gill passage. Data were standardized to a gill weight of 0.02 g. For statistical analysis a non-paired student's t-test was employed comparing the percentage decrease of the initial ammonia concentration during one passage through the gills in two different conditions. B) Calculated branchial ammonia excretion rate. Data were collected from the experiment where gills were perfused with 200 µmol L^{-1} and 500 µmol L^{-1} ammonia originated from 18 posterior

gills excised from 9 crabs (n = 9) and 61 gills excised from 24 crabs (n = 24), respectively. For statistical analysis a non-paired student's t-test was employed comparing the ammonia excretion rate in two different conditions. " * " indicates statistical significance with $p < 0.05$. Data was presented as mean ± SEM.

3.2. Regulation of branchial ammonia excretion *via* the cAMP/PKA pathway

3.2.1. Effects of the adenylate cyclase activator forskolin and membrane permeable 8-Bromo-cAMP on the branchial ammonia excretion rate

Under a transbranchial outwardly directed ammonia gradient (200 : 0 µmol L^{-1}), the basolateral application of forskolin (10 µmol L^{-1}) or 8-Bromo-cAMP (10 µmol L^{-1}) caused a complete halt of ammonia excretion. In addition, some metabolically produced ammonia was now transported towards the hemolymph side, enriching the initial ammonia concentration from 200 µmol L^{-1} to 216.5 ± 12.6 µmol L^{-1} and 205.2 ± 11.7 µmol L^{-1}, respectively, during a single passage through the gill (data not shown). Effects of both substances were fully (Fig. 7 A) and partial (Fig. 7 B) reversible in the wash-out step, indicating the viability of the gill.

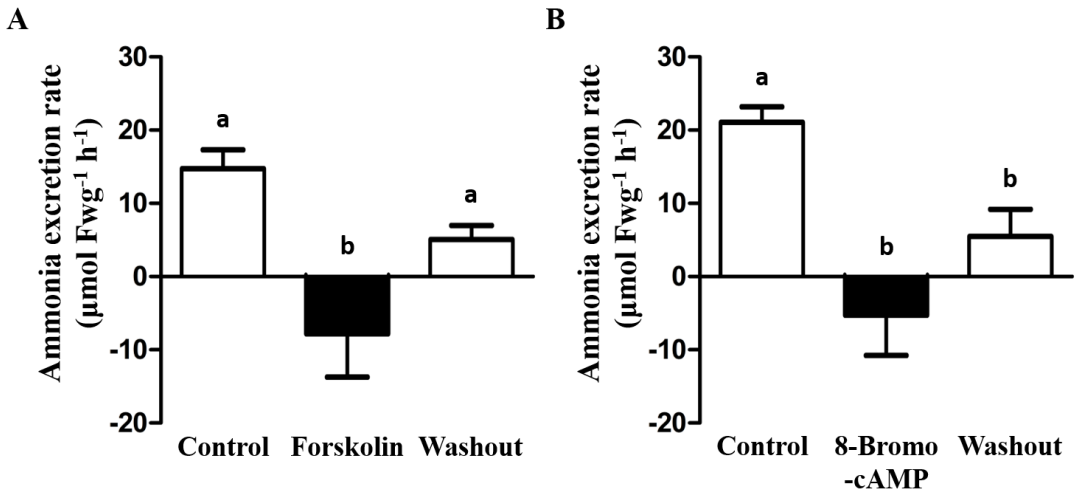

Figure 7. The effect of forskolin and 8-Bromo-cAMP on the branchial ammonia excretion in the posterior gills of *C. maenas* under an 200 : 0 µmol L^{-1} outwardly directed ammonia gradient. Gills were perfused with 200 µmol L^{-1} ammonia while bathed in a solution that contained no ammonia at the beginning of the experiment. A) Effect of basolateral applied forskolin (10 µmol L^{-1}). Data were collected and analyzed from 6 gills excised from 5 crabs (n = 5). B) Effect of basolateral applied 8-Bromo cAMP (10 µmol L^{-1}). Negative values reflect not an excretion of ammonia, but an enrichment of the perfusion saline with metabolically produced ammonia. Data

were collected and analyzed from 7 gills excised from 5 crabs (n = 5). Statistical significances were determined by using one-way Anova (repeated-measures, $p < 0.05$). Data are presented as mean ± SEM.

When a transbranchial outwardly directed ammonia gradient of 500 : 0 µmol L^{-1} was applied, basolateral application of forskolin (10 µmol L^{-1}) or the addition of 8-Bromo-cAMP (10 µmol L^{-1}) caused a *ca*. 74.3% and *ca*. 46.3% reduction of the ammonia excretion rate, respectively. As seen before, effects of both substances were partial reversible in the wash-out step (Fig. 8 A, B).

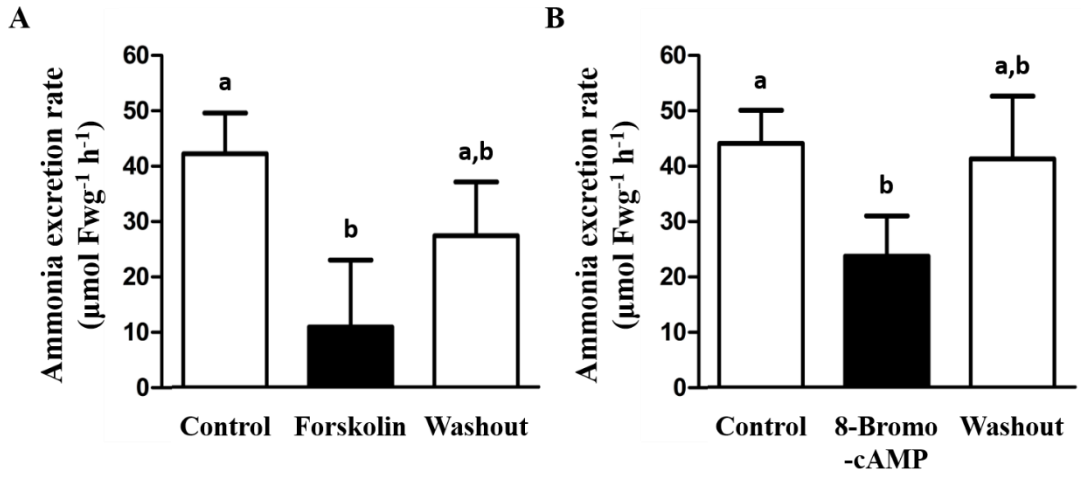

Figure 8. The effect of forskolin and 8-Bromo-cAMP on the branchial ammonia excretion in the posterior gills of *C. maenas* under 500 : 0 µmol L^{-1} outwardly directed ammonia gradient. Gills were perfused with 500 µmol L^{-1} ammonia while bathed in a solution that contained no ammonia at the beginning of the experiment. A) Effect of basolateral applied forskolin (10 µmol L^{-1}). Data were collected and analyzed from 7 gills excised from 5 crabs (n = 5). B) Effect of basolateral applied 8-Bromo cAMP (10 µmol L^{-1}). Data were collected and analyzed from 9 gills excised from 5 crabs (n = 5). Statistical significances were determined by using one-way Anova (repeated-measures, $p < 0.05$). Data are presented as mean ± SEM.

3.2.2. Effect of 8-Bromo-cAMP on metabolically produced branchial ammonia release

The previous experiment indicate that cAMP caused an increase in metabolic ammonia production (Fig. 7 B). To verify this result and to explore potential shifts in ammonia release directions, gills were now perfused and bathed in solutions that contained no ammonia.

When 8-Bromo-cAMP (10 µmol L^{-1}) was applied to the basolateral side, total ammonia produced by the gill metabolism increased by *ca*. 27.7 % which translates to an increase of the branchial release rate by 4.5 ± 1.3 µmol Fwg^{-1} h^{-1} (Fig. 9 A). All of the additional produced ammonia under the influence of 8-Bromo-cAMP was now released towards the hemolymph side, while no changes were observed in the ammonia release rate towards the apical side (Fig. 9 B, C). In addition, the apical to basolateral release ratio reversed from *ca.* 56.7 *vs.* 43.3 to 43.7 *vs.* 56.3 after application of 8-Bromo-cAMP (Fig. 9 D).

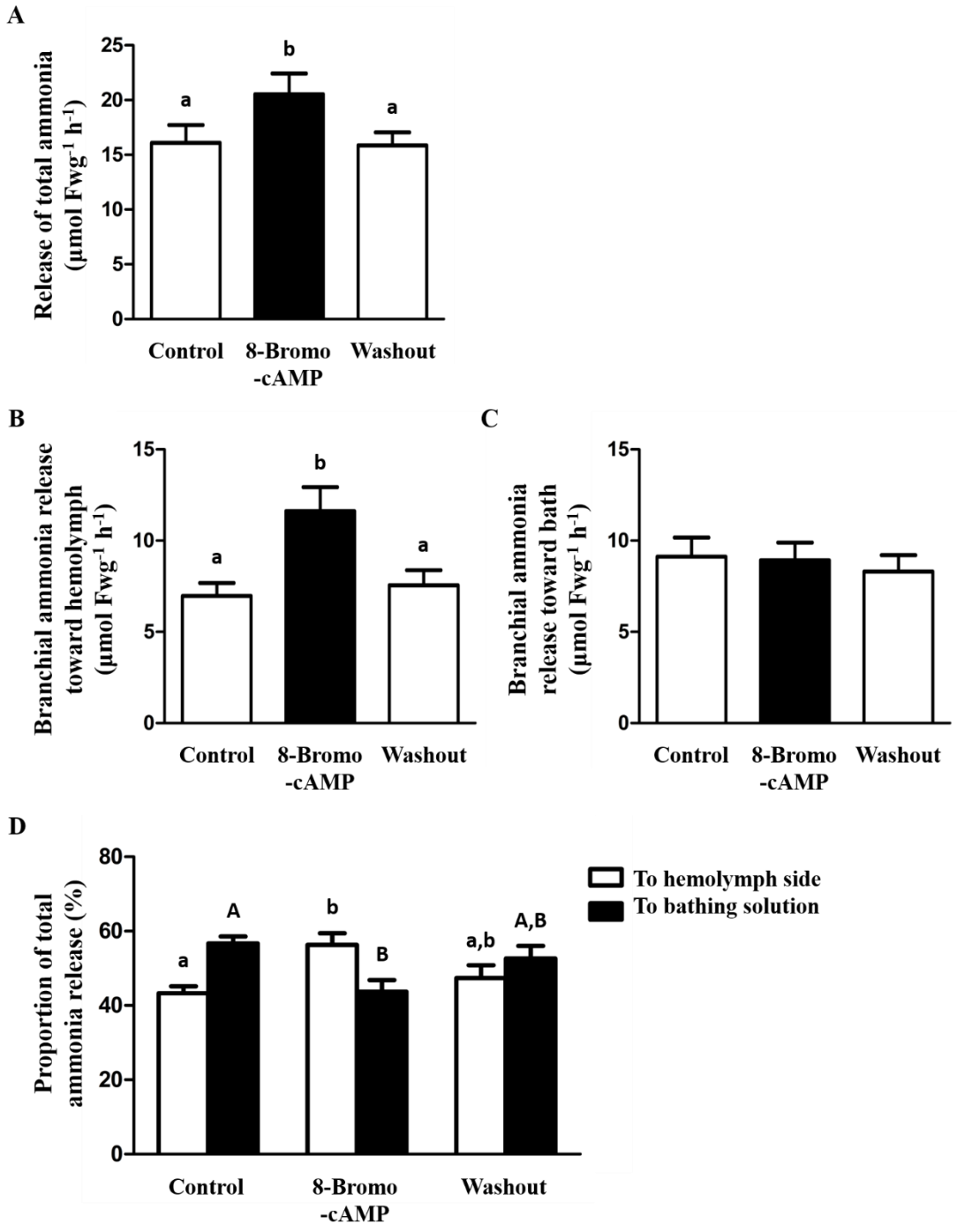

Figure 9. Metabolic ammonia release rate in the posterior gills of *C. maenas* after application of 10 µmol L^{-1} 8-Bromo-cAMP. No ammonia was present in the perfusion and bathing solution at the beginning of each experimental step. A) Total metabolic ammonia release rate. B) Metabolic ammonia release rate towards hemolymph side. C) Metabolic ammonia release rate towards the bathing solution. D) Ratio of branchial produced ammonia that is released towards the hemolymph side (white bar; differences were denoted in lower case letters) versus the bathing solution (black bar; differences were denoted in upper case letters). Data were collected and analyzed from 13 gills excised from 5 crabs (n = 5). Statistical significances were determined by using one-way Anova (repeated-measures, $p < 0.05$). Data are presented as mean ± SEM.

3.2.3. Baseline activity of the membrane-bound adenylyl cyclase and protein kinase A (PKA)

Crabs employed in this study were acclimated to brackish water conditions and gills were accordingly perfused (see methods). It has been shown in previous studies that under these conditions, gills from *C. maenas* display an active, maybe cAMP activated Na^+/K^+-ATPase-dependent branchial NaCl uptake suggested by the fact that isolated gills can switch between an osmoregulatory inactive to an osmoregulatory active state without external, e.g. hormonal, signals (Siebers et al., 1985). This suggests that Na^+/K^+-ATPase stimulating pathways, e.g. the cAMP/PKA pathway, may already be activated to a certain extent just by a low environmental salinity alone. To test whether the cAMP producing membrane-bound adenylyl cyclase or the cAMP-dependent PKA are already active in the control experiments of this study, the membrane adenylyl cyclase inhibitor SQ22536 (10 µmol L^{-1}) and PKA inhibitor KT5720 (250 nmol L^{-1}) were applied. As seen in figure 10 A & B, the application of any the above inhibitors had no effect on the branchial ammonia excretion rates, suggesting that under control conditions cAMP levels are low (not activating concentrations) and that the PKA is not active to an extent that influences ammonia excretion.

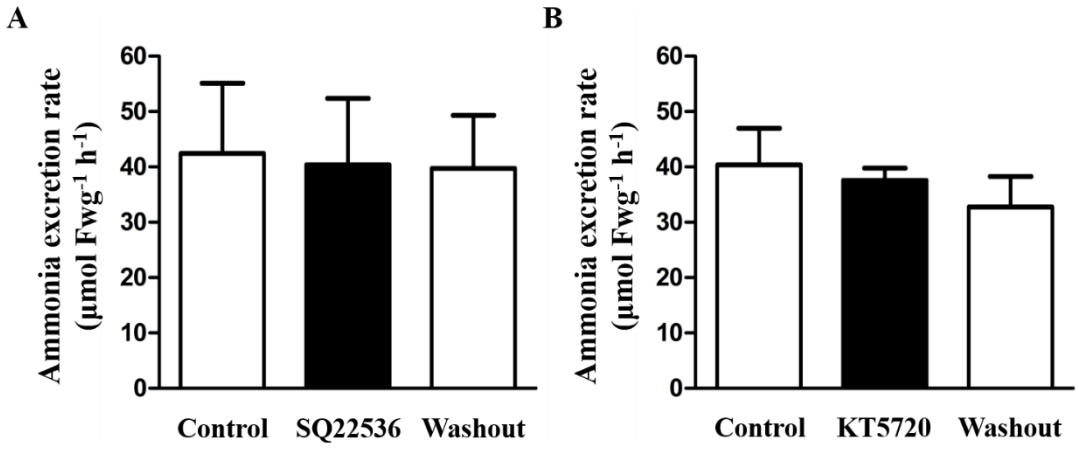

Figure 10. The effect of the membrane adenylyl cyclase inhibitor SQ22536 and PKA inhibitor KT5720 on the branchial ammonia excretion in the posterior gills of *C. maenas*. Gills were perfused with 500 µmol L^{-1} ammonia while bathed in a solution that contained no ammonia at the beginning of the experiment. A) Effect of 10 µmol L^{-1} SQ22536 on branchial ammonia excretion. Data were collected and analyzed from 6 gills excised from 3 crabs (n = 3). B) Effect of 0.25 µmol L^{-1} KT5720 on branchial ammonia excretion. Data were collected

and analyzed from 8 gills excised from 4 crabs (n = 4). Statistical significances were determined by using one-way Anova (repeated-measures). Data are presented as mean ± SEM.

3.3. Regulation of branchial ammonia excretion *via* the cGMP/PKG pathway

3.3.1. Effects of 8-Bromo-cGMP on branchial metabolic ammonia release

Since cAMP caused an increase in metabolic ammonia production, also the effects of the cyclic nucleotide second messenger, guanosine 3',5'-cyclic monophosphate (cGMP) on the metabolic ammonia production in *C. maenas* were investigated.

When 5 µmol L^{-1} of the membrane permeable cGMP analog, 8-Bromo-cGMP was applied, the rate of metabolically produced ammonia slightly decreased by *ca*. 15.7% from 16.3 ± 1.3 µmol Fwg^{-1} h^{-1} to 13.7 ± 0.8 µmol Fwg^{-1} h^{-1} (Fig. 11 A). These data, however, must be viewed with caution as the activity of the branchial epithelium of *C. maenas*, measured e.g. as the active ammonia excretion rate over the perfused gill, also decreases over time by *ca*. 16.3% per hour (Weihrauch, 1995). At the same time, the application of 8-Bromo-cGMP caused a less pronounced decrease of apically released ammonia, while a smaller amount of ammonia is now released towards the hemolymph side (Fig. 11 B, C). Overall, 8-Bromo-cGMP caused that a significant higher portion, 65.9% instead of 59.6%, of metabolically produced ammonia is released towards the apical bath (Fig. 11 D).

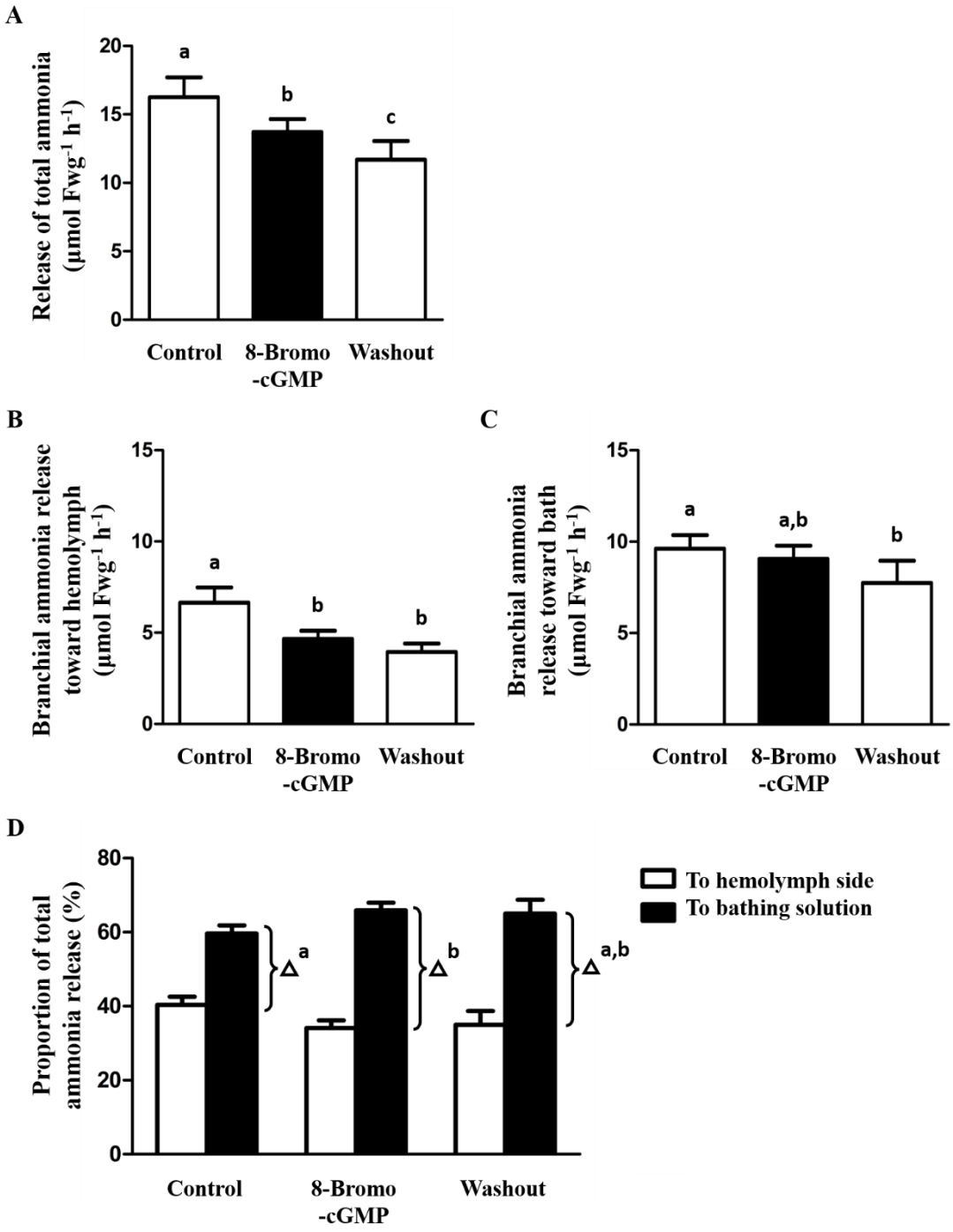

Figure 11. Metabolic ammonia release rate in the posterior gills of *C. maenas* after application of 5 µmol L^{-1} 8-Bromo-cGMP. No ammonia was present in the perfusion and bathing solution at the beginning of each experimental step. A) Total metabolic ammonia release rate. B) Metabolic ammonia release rate towards hemolymph side. C) Metabolic ammonia released towards the bathing solution. D) Ratio (in percent) of branchial produced ammonia that is released towards the hemolymph side (white bar) versus the bathing solution (black bar). "Δ" reflects the difference in the percentage release of metabolically produced ammonia towards the bathing solution and hemolymph, respectively. Data were collected and analyzed from 12 gills excised from 5 crabs (n = 5). Statistical significances were determined by using one-way Anova (repeated-measures, $p < 0.05$). Data are presented as mean ± SEM.

3.3.2. Effects of 8-Bromo-cGMP on the branchial ammonia excretion rate

Under the conditions of a 200 : 0 µmol L^{-1} and 500 : 0 µmol L^{-1} ammonia outwardly directed gradient, basolateral application of 5 µmol L^{-1} of 8-Bromo-cGMP caused an increase of the branchial excretion rate by 49.9% (p = 0.0961 in paired t-test) and 19.3%, respectively. It is of interest to note that under both conditions the absolute increase in excretion were similar with 8.3 µmol Fwg^{-1} h^{-1} and 7.8 µmol Fwg^{-1} h^{-1}, respectively. The effect of cGMP was reversed following the wash-out step (Fig. 12 A, B).

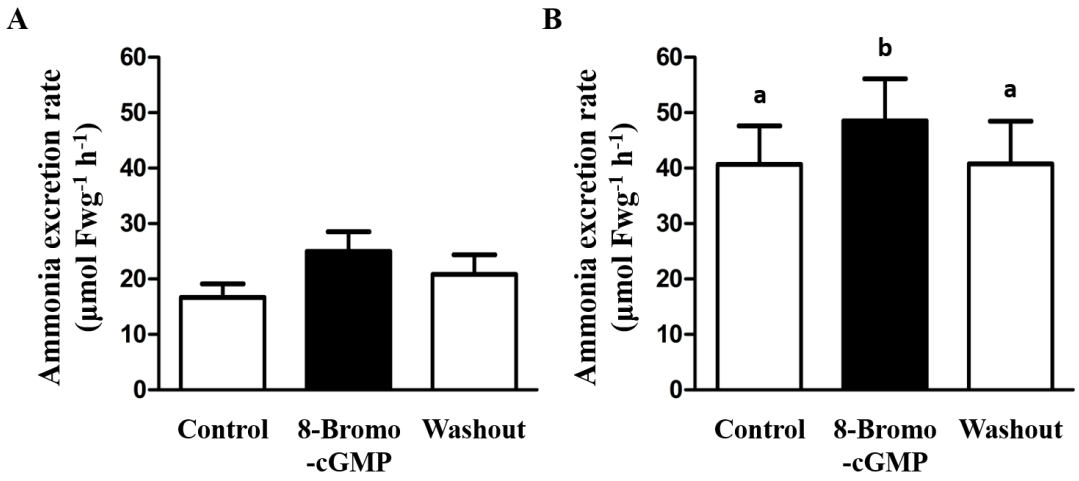

Figure 12. The effect of 5 µmol L^{-1} 8-Bromo-cGMP on the branchial ammonia excretion in the posterior gills of *C. maenas*. Gills were perfused with 200 µmol L^{-1} ammonia (A) or 500 µmol L^{-1} ammonia (B) while bathed in a solution that contained no ammonia at the beginning of the experiment. Data were collected and analyzed from 5 gills excised from 4 crabs for 200 : 0 µmol L^{-1} gradient (n = 4), and from 9 gills excised from 5 crabs for 500 : 0 µmol L^{-1} gradient (n = 5). Statistical significances were determined by using one-way Anova (repeated-measures, $p < 0.05$). Data are presented as mean ± SEM.

3.3.3. Effects of blocking protein kinase G (PKG) on the branchial ammonia excretion rate

The participation of protein kinase G (PKG) in the regulatory process of branchial ammonia excretion in *C. maenas* was investigated by employing the PKG inhibitor KT5823 (0.5 µmol L^{-1}). Inhibition of the PKG by KT5823 in the non-activated branchial epithelium caused a decrease of the excretion rate by 27.0% (Fig. 13 A) when an 500 : 0 µmol L^{-1}

outwardly directed ammonia gradient was applied. Moreover, when the gill tissue was pre-incubated with KT5823 (0.5 µmol L^{-1}), basolateral application of 8-Bromo-cGMP did not show the previously observed activating effect (Fig. 13 B).

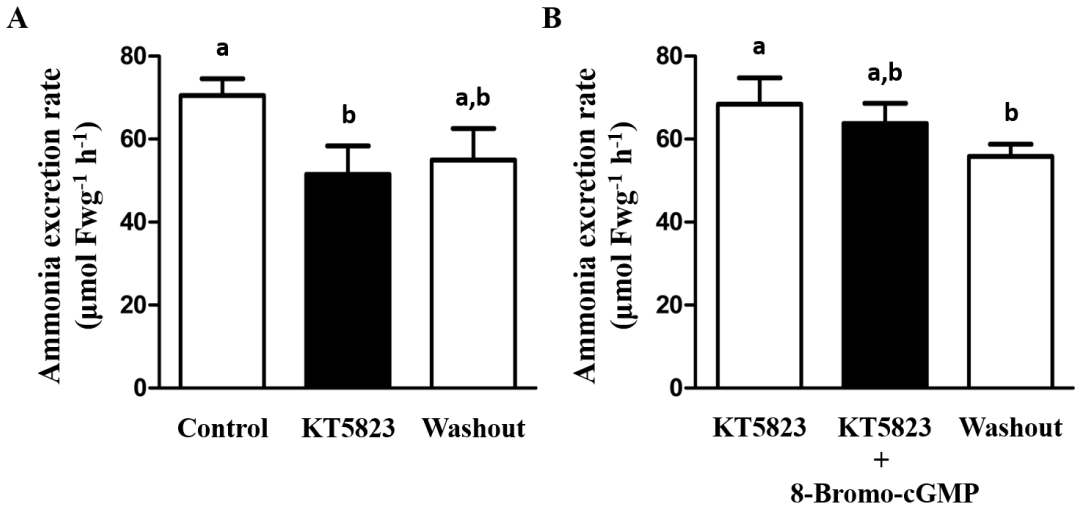

Figure 13. The effect of the PKG inhibitor KT5823 (0.5 µmol L^{-1}) on branchial ammonia excretion in the posterior gills of *C. maenas*. Gills were perfused with 500 µmol L^{-1} ammonia while bathed in a solution that contained no ammonia at the beginning of the experiment. A) Data were collected and analyzed from 6 gills excised from 5 crabs (n = 5). B) The effect of 8-Bromo-cGMP (5 µmol L^{-1}) on KT5823 pre-incubated gills. Data were collected and analyzed from 9 gills excised from 5 crabs (n = 5). Statistical significances were determined by using one-way Anova (repeated-measures, $p < 0.05$). Data are presented as mean ± SEM.

3.4. Participation of the nitric oxide pathway in branchial ammonia excretion

Besides cGMP production *via* a membrane-bound guanylyl cyclase (pGC), the soluble guanylyl cyclase (sGC), which is known to be activated *via* nitric oxide (NO) (Sürmeli et al., 2015), could provide cytoplasmatic cGMP and thereby play a role in regulating transbranchial ammonia excretion. In a first step, presence of pGC, sGC, and the NO producing nitric oxide synthase (NOS) mRNA in the gill tissue was verified by endpoint PCR (Fig. 14) employing gene specific primers (see table 1).

In gill perfusion experiments employing an 500 : 0 µmol L^{-1} outwardly directed ammonia

gradient inhibition of NOS with 1 mmol L^{-1} L-NG-nitroarginine methyl ester (L-NAME), caused a decrease of the ammonia excretion rate by 24.0% from 54.8 ± 5.6 to 41.7 ± 7.7 µmol Fwg^{-1} h^{-1}. This inhibition was off-set when in addition to the L-NAME inhibition 5 µmol L^{-1} 8-Bromo-cGMP was added to the perfusion solution, resulting in a transport rate of 56.2 ± 4.8 µmol Fwg^{-1} h^{-1} (Fig. 15).

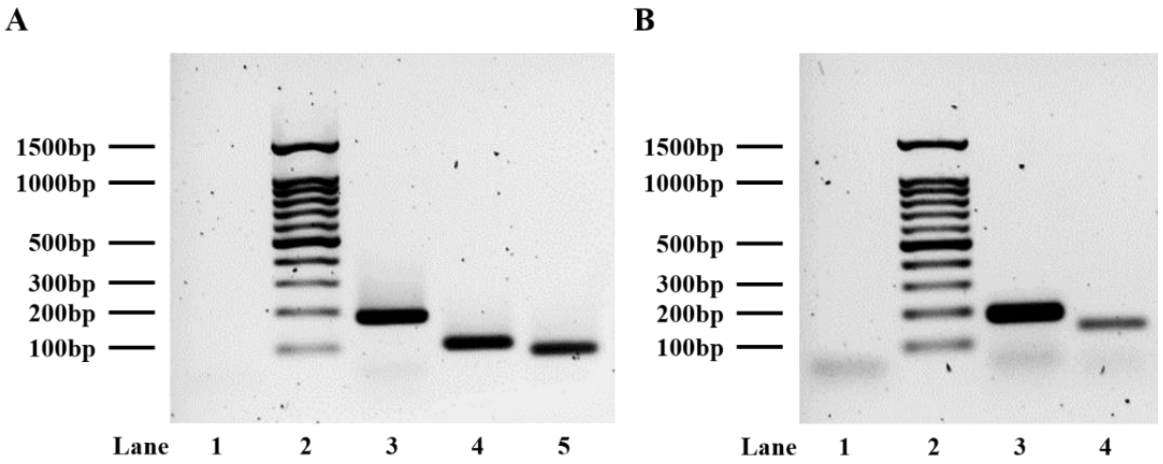

Figure 14. Ethidium bromide-stained agarose gel of PCR products (NOS, pGC, sGC) obtained from cDNA of posterior gills of *C. maenas*. A) Lane 1, negative control (no template); Lane 2, molecular weight marker; Lane 3, primers employed targeting arginine kinase (pos. ctr., predicted product size: 200 bp); Lane 4, primers employed targeting NOS (predicted product size: 116 bp); Lane 5, primers employed targeting pGC (predicted product size: 102 bp). B) Lane 1, negative control (no template); Lane 2, molecular weight marker; Lane 3, primers employed targeting arginine kinase (pos. ctr., predicted product size: 200 bp); Lane 4, primers employed targeting sGC (predicted product size: 147 bp).

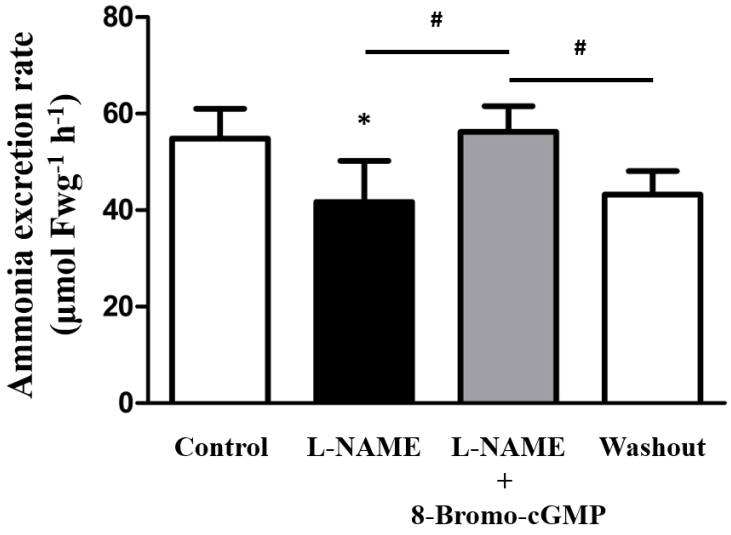

Figure 15. The effect of the NOS inhibitor L-NAME (1 mmol L^{-1}) on the branchial ammonia excretion in the posterior gills of *C. maenas*. Gills were perfused with 500 μmol L^{-1} ammonia while bathed in a solution that contained no ammonia at the beginning of the experiment. After basolateral application of 1 mmol L^{-1} L-NAME, 5 μmol L^{-1} 8-Bromo-cGMP were added additionally in a consecutive step. Data were collected and analyzed from 10 gills excised from 5 crabs (n = 5). Statistical significances were determined by using a paired t-test. " * " indicates statistical significance comparing to control with $p < 0.05$; " # " indicates statistical significance between two treatments with $p < 0.05$. Data was presented as mean ± SEM.

4. Discussion

In this study, ammonia excretion rates were measured in gills of *C. maenas* when either perfused with 200 µmol L^{-1} or 500 µmol L^{-1} ammonia (Fig. 6), with expected significant higher rates observed when a 500 µmol L^{-1} (hemolymph side) : 0 µmol L^{-1} (bath) ammonia gradient was applied. This finding is in accordance with results from a previous study on brackish water acclimated *C. maenas*. In fact, the former study revealed that in the physiological range of 50 – 800 µmol L^{-1} hemolymph ammonia, the majority of the branchial ammonia excretion was saturable and thereby transporter-dependent with a calculated K_t value of 301 µmol L^{-1} ammonia (Weihrauch et al., 1998). Under an outwardly directed gradient of 800 µmol L^{-1} ammonia (hemolymph): 0 µmol L^{-1} ammonia (bath) only *ca.* 29% of the excreted ammonia passed the gill epithelium *via* membrane diffusion (NH_3) or along the paracellular pathway over this moderate leaky gill epithelium (Weihrauch et al., 1998). When facing outwardly ammonia gradients (higher ammonia level in hemolymph), ammonia is transported by both passive (e.g. K^+ -channels, Rh-proteins) and active/secondary active (Na^+/K^+-ATPase, V-ATPase, vesicular transport) means (Weihrauch et al., 2002). The basolateral localized Na^+/K^+-ATPase plays a critical role in the excretory process as it accepts NH_4^+ as a substrate moving ammonia from the hemolymph into the cytoplasm (Leone et al., 2017). Blocking this pump by the specific Na^+/K^+-ATPase inhibitor ouabain reduced the passive (200 µmol L^{-1} ammonia on hemolymph side: 0 µmol L^{-1} ammonia in the apical bath) and active (100 µmol L^{-1} ammonia applied symmetrically) branchial ammonia excretion in *C. maenas* by *ca.* 52 and 60%, respectively (Weihrauch et al., 1998). Accordingly, it was unexpected to find that activation of the cAMP/PKA pathway by addition of 8-Bromo-cAMP did not cause an increase in branchial ammonia excretion, but ammonia retention (see Fig. 7). In contrast, the current study revealed that the NO/cGMP/PKG pathway activated ammonia excretion in the gills of the *C. maenas* (see Fig. 16).

4.1. Participation of the NO/cGMP/PKG pathway in regulating ammonia excretion

Blocking PKG by applying the PKG inhibitor KT5823 without previously activating the gill epithelia cells *via* cGMP resulted in a *ca*. 27% decrease in ammonia excretion, suggesting a certain baseline activity of the PKG pathway (Fig. 13 A). In support of this finding, the application of KT5823 eliminated the effect of cGMP on branchial ammonia excretion, further implying a role of PKG in the activation process (Fig. 13 B). Participation of the cGMP/PKG pathway in branchial ammonia excretion was indirectly suggested in an earlier study where the application of the crustacean hyperglycemic hormone (CHH) resulted in an increased excretion rate in *C. maenas* gills (Fehsenfeld et al., 2023a), while the CHH binding site was suggested to be coupled to a second messenger system involving cGMP (Chung and Webster, 2006). In the current study, the effects of cGMP on metabolically produced ammonia were only minor. In fact, considering a slowing metabolic production rate over time in perfused *C. maenas* gills by *ca.* 16.3% per hour (Weihrauch, 1995) due to cellular decay inevitable in this preparation, no effect must be reported upon the application of cGMP. Nonetheless, and independently of a decay of excretion over time, a significant shift to a greater proportion of produced ammonia release towards the apical bath was observed (Fig. 11 D).

Another important finding in this study is the involvement of NOS. This indicates that NO as a second messenger plays part in the branchial ammonia excretion process. As a NOS inhibitor, L-NAME is hydrolyzed into L-NOARG, competing with L-arginine and inhibiting the production of NO (Peter and Gayathry, 2021; Reif and McCreedy, 1995). The decrease of the ammonia excretion rate under the influence of L-NAME indicates that NOS and NO were involved in the ammonia excretion process in the gills (Fig. 15). Note, in living animals NO, a gaseous membrane permeable molecule, is either produced by the target cell itself or diffuses into the target cell from adjacent cells and vessels. Since experiments were performed using isolated gills, the sole source of NO was considered to be the result of branchial NOS activity. This assumption is supported by the finding that NOS transcripts were found in the gill epithelium of *C. maenas* by endpoint PCR (Fig. 14 A). Cellular NO is known to activate sGC

(Ridgel et al., 2012). Once activated by NO upon binding, the increased activity of sGC leads to a higher production of cellular cGMP (Fig. 16). This has been e.g. shown in a previous study where an incubation with 1 mmol L^{-1} of Diethylamine NONOate (a donor of NO) caused a 300-fold increase of cGMP formation in heart tissues of rats (Mayer et al., 1998).

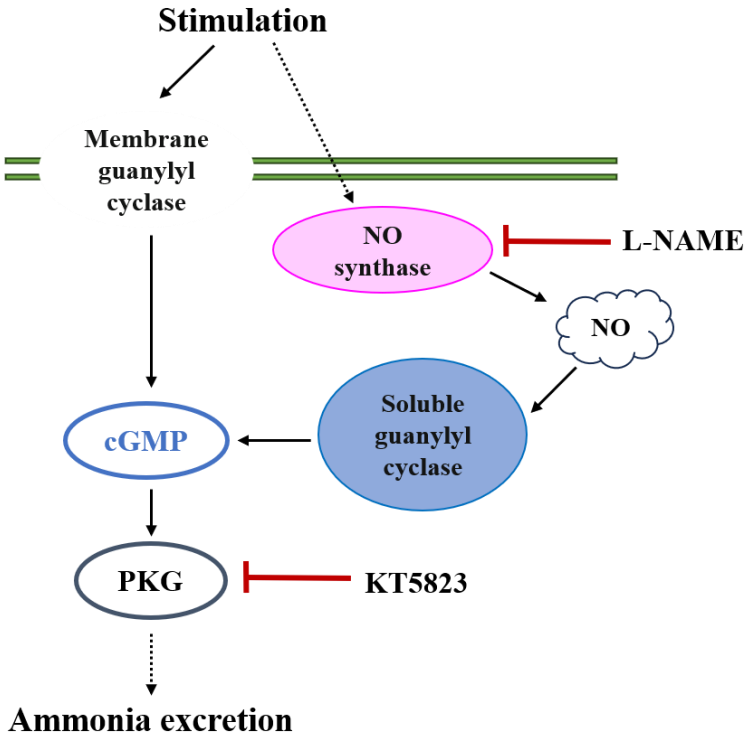

Figure 16. Predicted pathways for the NO/cGMP/PKG in regulating the ammonia excretion in the posterior gills of *C. maenas*. Note, participation of the membrane bound GC has not been confirmed yet as it is activated by a so far not-confirmed extracellular signal, possibly the hormone CHH. Presence of NOS, sGC, and pGC has been confirmed in the branchial epithelium of *C. maenas* (Fig. 14).

Interestingly, in spite of the larger applied ammonia gradient (500 µmol L^{-1} : 0 µmol L^{-1} *vs*. 200 µmol L^{-1} : 0 µmol L^{-1}), the actual increase of the ammonia excretion rate was comparable after the application of cGMP, and measured to 7.8 and 8.3 µmol Fwg^{-1} h^{-1}, respectively (Fig. 12). Since this promotion of excretion was not greatly influenced by the differences of the applied ammonia gradient, it is considered to be related solely to the transporter-mediated ammonia transport instead of ammonia diffusion (membrane or paracellular), probably by an excretory pathway that is running at its maximum under cGMP

activation already at the smaller outwardly directed ammonia gradient. However, the final target of the activated PKG is not clear and will be a topic of follow-up studies. A potential candidate may be the V-ATPase, which may be potentially regulated by cGMP activation as shown in the Malpighian tubules of the fruit fly *Drosophila melanogaster* (O'Donnell et al., 1996). As mentioned in the introduction, the V-ATPase is crucial for the active ammonia excretion but not involved in osmoregulatory NaCl uptake in the gills of *C. maenas* (Weihrauch et al., 2001). Furthermore, in vertebrate systems, PKG has a regulatory effect on transporters, such as Na^+/K^+-ATPase, K^+-channels, and cation proton exchangers, all transporters that have also been shown to play a role in ammonia excretion in fish and aquatic invertebrates (Fehsenfeld et al., 2019; Fehsenfeld and Weihrauch, 2016; Weihrauch et al., 1998).

Notably, cGMP functions as an activator of PKG, but it has its own ability in activating cyclic nucleotide–gated ion channels through direct binding to the intracellular sites (Kaupp and Seifert, 2002). This process may change the membrane permeability to Ca^{2+}, leading to a Ca^{2+} influx, which is crucial for the activation of NOS (Schmidt et al., 1992).

4.2. Participation of the cAMP/PKA pathway in regulating ammonia retention

Cyclic AMP was shown to have an effect in perfused gills of the osmoregulating *C. granulatus* when applied to the basolateral membrane where 10 µmol L^{-1} of the cAMP analogue, cp-cAMP, caused a nearly 10-fold increase in the transepithelial potential difference (PD_{te}), indicating an increase in branchial NaCl uptake, which depends directly on the activity of Na^+/K^+-ATPase (Luquet et al., 2002). Further, the application of forskolin, an activator of the adenylate cyclase, caused a similar increase of the PD_{te} as observed under the addition of cp-cAMP, while activating the Na^+/K^+-ATPase activity by *ca.* 50% (Halperin et al., 2004).

As mentioned earlier, Na^+/K^+-ATPase has been shown to play a crucial role in the excretory mechanism of ammonia in many invertebrates and fish (Durant and Donini, 2019; Weihrauch et al., 2012; Wright and Wood, 2012).

Under the impact of ouabain, a specific inhibitor of Na^+/K^+-ATPase, active brachial

ammonia excretion in the *M. magister* ceased, while ammonia produced by the gills was released towards the hemolymph side (Allen et al., 2024). In *C. maenas* basolateral application of ouabain led to a *ca.* 60% reduction of the active ammonia excretion (Weihrauch et al., 1998). Due to its demonstrated participation in branchial excretory mechanisms, an increase of branchial ammonia excretion in *C. maenas* was expected upon activation by the cAMP/PKA pathway. However, the current study demonstrated a retention of ammonia even when an outwardly directed ammonia gradient was applied (see Fig. 7). In fact, with a 200 : 0 µmol L^{-1} outwardly directed ammonia gradient applied over the gill epithelium, 8-Bromo-cAMP caused a complete cessation of the transbranchial excretion, while metabolic ammonia, likely due to the now higher energy demand of activated Na^+/K^+-ATPase (Halperin et al., 2004), was enhanced by 5.3 ± 4.9 µmol Fwg^{-1} h^{-1}. Interestingly, this "extra" produced ammonia was now transported towards the hemolymph side. This enhancement of metabolically produced ammonia was independent of the applied transbranchial ammonia gradient, as cAMP activation caused an increase (4.4 ± 1.3 µmol Fwg^{-1} h^{-1}) when no ammonia was provided on either side of the epithelium. Also in this experiment, all additional produced ammonia was released towards the hemolymph side, indicating the existence of a meaningful, so far unknown, but physiological relevant pathway.

It is noteworthy that the cAMP/PKA pathway, in contrast to the cGMP/PKG pathway, does not display any baseline activity under the experimental conditions, as the PKA specific inhibitor KT5720 but also the adenylyl cyclase inhibitor SQ22536 showed no effect on branchial ammonia excretion rate (see Fig. 10, 17).

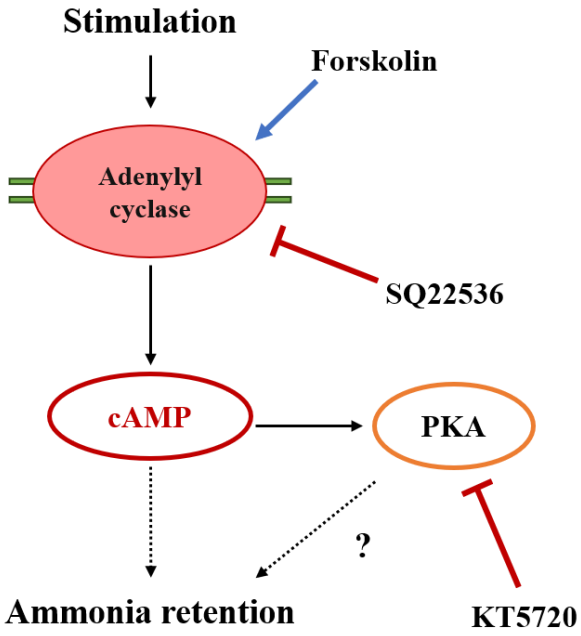

Figure 17. Predicted pathways for cAMP/PKA in regulating the ammonia excretion in the posterior gills of *C. maenas*. In the current study, increased levels of cAMP (either by adding 8-Bromo-cAMP directly or by activating membrane adenylyl cyclase) led to ammonia retention. However, the involvement of PKA in this process remains unclear.

Literature on cellular regulatory pathways for epithelial ammonia transport is in general very sparse. In line with the presented data are studies on the marine polychaete *Eurythoe complanata*. When exposed to 8-Bromo-cAMP, ammonia excretion of whole animals was significantly reduced. By contrast, when blocking the soluble adenylate cyclase with KH7 and lowering thereby cellular cAMP levels, ammonia excretion increased (Thiel et al., 2017). This is in contrast to findings in the common octopus *Octopus vulgaris*, where blood ammonia levels are kept relatively high (close to 300 µmol L^{-1}), when compared to fish (lower than 120 µmol L^{-1}, (Shin et al., 2016)), human (11 to 32 µmol L^{-1}, (Braissant et al., 2013)), or most of decapod crabs (80-200 µmol L^{-1}, (Weihrauch and McGaw, 2023)). When isolated *O. vulgaris* gills were perfused with 300 µmol L^{-1} NH_4^+, basolateral addition of 8-Bromo-cAMP or KH7 had no effect on the amount of metabolically produced ammonia released towards the environment (*ca.* 70% of total) and blood side (*ca.* 30% of total), respectively. However, when gills were perfused with a solution containing no ammonia, blocking the soluble adenylate cyclase with KH7 caused a decrease in apical excretion and an increase in basolateral release of metabolic

ammonia (Hu et al., 2017). Further, a study by Worrell and coworkers showed that forskolin promoted the serosal to mucosal NH_4^+ net transport in the human colonic carcinoma cell line T84 (Worrell et al., 2008). According to the authors, this transport depended on Na^+/K^+-ATPase and on a basolateral localized bumetanide-sensitive $Na^+/K^+/2Cl^-$ cotransporter (NKCC1), where NH_4^+ can substitute K^+ and being transported from the blood into the cytoplasm of the epithelial cell. An earlier study revealed that mammalian NKCC1 can indeed be activated by cAMP (Matthews et al., 1992). A $Na^+/K^+/2Cl^-$ cotransporter was also identified, by molecular means, in the gills of *C. maenas* (Towle and Weihrauch, 2001) and was suggested to be situated in the apical membrane and to play a key role in NaCl uptake (Riestenpatt et al., 1996). It is, however, unlikely that this NKCC, even when in theory activated by cAMP can explain the observed retention of ammonia as no NH_4^+ as a potential substrate was available in the conducted experiment.

Lastly, a study on the African clawed frog *Xenopus laevis* showed that the transcutaneous net ammonia excretion more than doubled following an application of theophylline (1,3-dimethylxanthine), an inhibitor of phosphodiesterase (Cruz et al., 2013). It was suggested, but not measured, that theophylline caused an increase of intracellular cAMP levels. It is also conceivable that theophylline, as a non-specific inhibitor of phosphodiesterase enzymes, may also cause an increase of cellular cGMP levels (Barnes, 2013), which in turn may promote cutaneous ammonia excretion in the frog.

As mentioned in the introduction, ammonia is a highly toxic molecule that needs to be either detoxified into less dangerous molecules such as urea (mammals, adult amphibians) and uric acid (all other land-living animals) or excreted out of the body fluids (Weihrauch et al., 2004b). With only a handful of known exceptions all aquatic living animals (fish and all invertebrates) do excrete ammonia as is, exhibiting a highly effective ammonia excretion mechanism in the excretory tissues, often across the gills or skin (Larsen et al., 2014; Quijada-Rodriguez et al., 2015).

This begs the question of why, some animals feature fairly high, potentially toxic, ammonia concentrations within their body fluids. Some land-locked insect larvae, e.g. the tobacco hornworm *M. sexta*, exhibit fast growth rates, while feeding on a nitrogen-poor diet.

These animals are in fact capable of utilizing ammonia directly for amino acid synthesis, crucial for growth and feature an active ammonia uptake in the midgut. Here hemolymph ammonia was measured to 0.8 ± 0.1 mmol L^{-1} (Weihrauch, 2006). In other cases, the reason for keeping elevated systemic ammonia concentrations is not clear and has not been investigated so far. For instance, in the hydrothermal vent crab *Xenograpsus testudinatus*, adapted to an extreme hypercapnic environment, a hemolymph ammonia concentration of 1.2 to 1.4 mmol L^{-1} was observed, although ammonia concentration in their respective environment is very low (Allen et al., 2020). As a marine invertebrate, *X. testudinatus* is ammontelic, excreting metabolically produced ammonia across the gill epithelium. The observed exceptionally high ammonia concentration found in the hemolymph of this crab - other aquatic decapod crustaceans feature *ca.* 50 – 200 µmol L^{-1} (Weihrauch et al., 2017) – implies the existence of mechanisms to intentionally maintain hemolymph ammonia at a high level rather than excreting the toxic molecule. As *X. testudinatus* lives in an extreme acid-base challenging environment with partial pressures of CO_2 ranging between 2.8 and 24.6 kPa (Allen et al., 2020), one can speculate that ammonia functions as an important acid-base equivalent, which can be either moved in its acidic form, NH_4^+, utilizing e.g. Na^+/K^+-ATPase (Wall, 1996), HIAT1 (Fehsenfeld et al., 2023b), or in its gaseous state (weak base) NH_3, e.g. by the branchial expressed Rh-protein (Quijada-Rodriguez et al., 2024).

In fact, when *C. maenas* crabs were exposed to elevated environmental pCO_2 levels of 1000 Pascals for 48 h, hemolymph pH values deceased only slightly by 0.11 units, while hemolymph ammonia concentrations quadrupled to *ca.* 400 µmol L^{-1} (Fehsenfeld and Weihrauch, 2015).

4.3. Interplay between the NO/cGMP/PKG and cAMP/PKA pathway

In this study, the NO/cGMP/PKG pathway and the cAMP/PKA pathway were investigated separately, however, cross-talk and interactions between these two pathways are commonly seen and should be considered. For example, in regulation of mammalian cardiac function, the cross-talk between the cAMP and cGMP signaling pathways requires the activity of the dual-

specificity phosphodiesterases (PDEs) (Calamera et al., 2022; Zaccolo and Movsesian, 2007). Depending on intracellular cGMP levels and the affinity differences among PDEs, intracellular cAMP could be either upregulated by inhibition of PDE3 (cGMP levels lower than 50 nmol L^{-1}) or downregulated by stimulation of PDE2 (cGMP levels between 200 to 500 nmol L^{-1}) (Zaccolo and Movsesian, 2007). Cross-talk also plays a role in crustaceans' response to hormone stimulation, e.g. by the crustacean hyperglycemic hormone (CHH). In the current experiments, no hormones were applied to the gills, yet the receptor for CHH is expressed in gill epithelium (Chung and Webster, 2006). Early studies have shown that cAMP and cGMP act as intracellular signaling messengers that mediate the action of CHH (Covi et al., 2009). CHH binds to the G protein-coupled receptor, activating adenylyl cyclase and membrane guanylyl cyclase, which in turn leads to increased levels of cAMP and cGMP, respectively (Chen et al., 2020). PKA activation induced by cAMP could phosphorylate a membrane Ca^{2+} channel, leading to an increase of intracellular calcium levels (Covi et al., 2012). At the following step, Ca^{2+} then binds to calmodulin, stimulating NOS and enhancing the production of endogenous NO. Nitric oxide in turn activates the soluble guanylyl cyclase within the cytoplasm, causing more cGMP production (Mo et al., 2024).

In other words, although highly complex, studies on cellular regulatory pathways should ideally be conducted under full consideration of the animals' circulating hormone pool and concentrations under various physiological conditions (e.g. feeding *vs*. non-feeding, acid-base challenges, etc.).

4.4. Conclusions and future studies

This study demonstrates for the first time directly that the cGMP/PKG signaling pathway promotes branchial ammonia excretion in an aquatic species, revealing new targets and candidates for investigating ammonia excretion process not just in crustaceans, but also in vertebrates, including fish and mammals (intestine, kidney). Gaining knowledge on that subject opens applications in the medical field, e.g. developing treatments of hyperammonemia, but also in aquaculture management and animal welfare, where large numbers of animals are forced to live in confinement, while their surrounding high ammonia concentrations. However, further

investigations are required to intentify the further downstream effecter of PKG in regulating ammonia excretion and the respective cellular targets in general in *C. maenas*. Further, investigating the status of phosphorylation of PKG upon internal or external ammonia loads or acid-base disturbances could be a valuable approach.

This study, also demonstrates clearly that animals have a controllable mechanism in place to retain elevated ammonia levels within their body fluids. To the author's knowledge, the function of elevated ammonia levels, particularly in aquatic animals have not been investigated yet. Accordingly, it has also not been studied in any system, by what kind of transporting mechanism and upon which trigger/regulation ammonia is released from the cytoplasm of the epithelial cells towards the body fluids. A candidate to facilitate this transport may be the hyperpolarization-activated cyclic nucleotide-gated K^+ channel (HCN). This K^+ channel has been shown to a) be localized in the basolateral membrane of *C. maeans* gill epithelia, b) involved in transbranchial ammonia excretion, c) mediated NH_4^+ transport (Fehsenfeld and Weihrauch, 2016), and d) be activated by cAMP (Porro et al., 2024).

Another candidate for basolateral ammonia release may be the Hippocampus abundant transcript 1 (Hiat1), a recently discovered, Na^+ -dependent NH_4^+ transporter (Fehsenfeld et al., 2023b). This transporter was suggested to serve as a housekeeping protein and can be found in all so far investigated tissues, including the gills of the *C. maeans*. The localization of Hiat1 has not been confirmed yet, however, if situated on the basolateral membrane, activation of Na^+/K^+-ATPase by cAMP, could drive NH_4^+ out of the cell into the hemolymph space.

Other possible targets for cAMP in regulating ammonia transport/retention are potentially the microtubule motor proteins, kinesin and dynein. Elevated cAMP levels in fish melanophores causing a inhibition of dynein activity during melanosomes dispersion whereas low cAMP level led to kinesin inactivation during the aggregation of melanosomes (Skold et al., 2002). Since the microtubule network and the movement of vesicles play important roles in ammonia transport in the crab gills (Weihrauch et al., 2002), increase of cAMP may regulate the ammonia excretion process *via* the activity of the motor proteins.

5. References

Abuhagr, A. M., Blindert, J. L., Nimitkul, S., Zander, I. A., Labere, S. M., Chang, S. A., Maclea, K. S., Chang, E. S. and Mykles, D. L. (2014). Molt regulation in green and red color morphs of the crab *Carcinus maenas*: gene expression of molt-inhibiting hormone signaling components. *J Exp Biol* **217**, 796-808.

Adlimoghaddam, A., O'Donnell, M. J., Kormish, J., Banh, S., Treberg, J. R., Merz, D. and Weihrauch, D. (2016a). Ammonia excretion in *Caenorhabditis elegans*: Physiological and molecular characterization of the *rhr-2* knock-out mutant. *Comp Biochem Physiol A Mol Integr Physiol* **195**, 46-54.

Adlimoghaddam, A., Sabbir, M. G. and Albensi, B. C. (2016b). Ammonia as a potential neurotoxic factor in Alzheimer's disease. *Front Mol Neurosci* **9**, 57.

Allen, G. J. P., Kuan, P. L., Tseng, Y. C., Hwang, P. P., Quijada-Rodriguez, A. R. and Weihrauch, D. (2020). Specialized adaptations allow vent-endemic crabs (*Xenograpsus testudinatus*) to thrive under extreme environmental hypercapnia. *Sci Rep* **10**, 11720.

Allen, G. J. P., Quijada-Rodriguez, A. R., Wilson, J. M. and Weihrauch, D. (2024). The role of the antennal glands and gills in acid-base regulation and ammonia excretion of a marine osmoconforming brachyuran. *Comp Biochem Physiol A Mol Integr Physiol* **292**, 111619.

Allen, G. J. P. and Weihrauch, D. (2021). Exploring the versatility of the perfused crustacean gill as a model for transbranchial transport processes. *Comparative Biochemistry and Physiology B-Biochemistry & Molecular Biology* **254**, 110572.

Alzamora, R., Thali, R. F., Gong, F., Smolak, C., Li, H., Baty, C. J., Bertrand, C. A., Auchli, Y., Brunisholz, R. A., Neumann, D. et al. (2010). PKA regulates vacuolar H^+-ATPase localization and activity via direct phosphorylation of the a subunit in kidney cells. *J Biol Chem* **285**, 24676-24685.

Barnes, P. J. (2013). Theophylline. *Am J Respir Crit Care Med* **188**, 901-906.

Bauer, P. J. (2002). The complex of cGMP-gated channel and Na^+/Ca^{2+}, K^+ exchanger in rod photoreceptors. In *Photoreceptors and Calcium. Advances in Experimental Medicine and*

Biology, vol. 514, pp. 253-274. Boston, MA: Springer.

Braissant, O., McLin, V. A. and Cudalbu, C. (2013). Ammonia toxicity to the brain. *J Inherit Metab Dis* **36**, 595-612.

Burgoyne, J. R., Prysyazhna, O., Rudyk, O. and Eaton, P. (2012). cGMP-dependent activation of protein kinase G precludes disulfide activation: implications for blood pressure control. *Hypertension* **60**, 1301-1308.

Butterworth, R. F. (2002). Pathophysiology of hepatic encephalopathy: a new look at ammonia. *Metab Brain Dis* **17**, 221-227.

Calamera, G., Moltzau, L. R., Levy, F. O. and Andressen, K. W. (2022). Phosphodiesterases and compartmentation of cAMP and cGMP signaling in regulation of cardiac contractility in normal and failing hearts. *Int J Mol Sci* **23**, 2145.

Cameron, J. N. and Heisler, N. (1983). Studies of ammonia in the rainbow trout physico-chemical parameters, acid-base behaviour and respiratory clearance. *J Exp Biol* **105**, 107-125.

Chen, H. Y., Toullec, J. Y. and Lee, C. Y. (2020). The crustacean hyperglycemic hormone superfamily: progress made in the past decade. *Frontiers in Endocrinology* **11**, 578958.

Cheng, C. H., Ma, H. L., Su, Y. L., Deng, Y. Q., Feng, J., Xie, J. W., Chen, X. L. and Guo, Z. X. (2019). Ammonia toxicity in the mud crab (*Scylla paramamosain*): The mechanistic insight from physiology to transcriptome analysis. *Ecotoxicol Environ Saf* **179**, 9-16.

Cheng, X., Ma, Y., Moore, M., Hemmings, B. A. and Taylor, S. S. (1998). Phosphorylation and activation of cAMP-dependent protein kinase by phosphoinositide-dependent protein kinase. *Proc Natl Acad Sci U S A* **95**, 9849-9854.

Chung, J. S. and Webster, S. G. (2006). Binding sites of crustacean hyperglycemic hormone and its second messengers on gills and hindgut of the green shore crab, *Carcinus maenas*: a possible osmoregulatory role. *Gen Comp Endocrinol* **147**, 206-213.

Covi, J. A., Chang, E. S. and Mykles, D. L. (2009). Conserved role of cyclic nucleotides in the regulation of ecdysteroidogenesis by the crustacean molting gland. *Comp Biochem Physiol A Mol Integr Physiol* **152**, 470-477.

Covi, J. A., Chang, E. S. and Mykles, D. L. (2012). Neuropeptide signaling mechanisms in crustacean and insect molting glands. *Invertebrate Reproduction & Development* **56**, 33-49.

Cruz, M. J., Sourial, M. M., Treberg, J. R., Fehsenfeld, S., Adlimoghaddam, A. and Weihrauch, D. (2013). Cutaneous nitrogen excretion in the African clawed frog *Xenopus laevis*: effects of high environmental ammonia (HEA). *Aquat Toxicol* **136-137**, 1-12.

Dames, P., Zimmermann, B., Schmidt, R., Rein, J., Voss, M., Schewe, B., Walz, B. and Baumann, O. (2006). cAMP regulates plasma membrane vacuolar-type H^+-ATPase assembly and activity in blowfly salivary glands. *Proc Natl Acad Sci U S A* **103**, 3926-3931.

Derbyshire, E. R. and Marletta, M. A. (2009). Biochemistry of soluble guanylate cyclase. In *cGMP: Generators, Effectors and Therapeutic Implications*, pp. 17-31. Berlin, Heidelberg: Springer.

Durant, A. C. and Donini, A. (2019). Development of *Aedes aegypti* (Diptera: Culicidae) mosquito larvae in high ammonia sewage in septic tanks causes alterations in ammonia excretion, ammonia transporter expression, and osmoregulation. *Sci Rep* **9**, 19028.

Fehsenfeld, S., Kolosov, D., Wood, C. M. and O'Donnell, M. J. (2019). Section-specific H^+ flux in renal tubules of fasted and fed goldfish. *J Exp Biol* **222**, jeb200964.

Fehsenfeld, S., Quijada-Rodriguez, A. R., Calosi, P. and Weihrauch, D. (2023a). The role of octopamine and crustacean hyperglycemic hormone (CHH) in branchial acid-base regulation in the European green crab, *Carcinus maenas*. *J Comp Physiol B* **193**, 509-522.

Fehsenfeld, S., Quijada-Rodriguez, A. R., Zhouyao, H., Durant, A. C., Donini, A., Sachs, M., Eck, P. and Weihrauch, D. (2023b). Hiat1 as a new transporter involved in ammonia regulation. *Sci Rep* **13**, 4416.

Fehsenfeld, S. and Weihrauch, D. (2013). Differential acid-base regulation in various gills of the green crab *Carcinus maenas*: Effects of elevated environmental pCO_2. *Comp Biochem Physiol A Mol Integr Physiol* **164**, 54-65.

Fehsenfeld, S. and Weihrauch, D. (2015). Mechanisms of acid–base regulation in seawater-acclimated green crabs (*Carcinus maenas*). *Canadian Journal of Zoology* **94**, 95-107.

Fehsenfeld, S. and Weihrauch, D. (2016). The role of an ancestral hyperpolarization-activated cyclic nucleotide-gated K^+ channel in branchial acid-base regulation in the green crab, *Carcinus maenas*. *J Exp Biol* **219**, 887-896.

Förstermann, U. and Sessa, W. C. (2012). Nitric oxide synthases: regulation and function.

Eur Heart J **33**, 829-837.

Francis, S. H., Busch, J. L., Corbin, J. D. and Sibley, D. (2010). cGMP-dependent protein kinases and cGMP phosphodiesterases in nitric oxide and cGMP action. *Pharmacol Rev* **62**, 525-563.

Francis, S. H., Poteet-Smith, C., Busch, J. L., Richie-Jannetta, R. and Corbin, J. D. (2002). Mechanisms of autoinhibition in cyclic nucleotide-dependent protein kinases. *Front Biosci* **7**, d580-d592.

Freire, C. A., Onken, H. and McNamara, J. C. (2008). A structure-function analysis of ion transport in crustacean gills and excretory organs. *Comp Biochem Physiol A Mol Integr Physiol* **151**, 272-304.

Gambaryan, S. (2022). The role of NO/sGC/cGMP/PKG signaling pathway in regulation of platelet function. *Cells* **11**, 3704.

Genovese, G., Senek, M., Ortiz, N., Regueira, M., Towle, D. W., Tresguerres, M. and Luquet, C. M. (2006). Dopaminergic regulation of ion transport in gills of the euryhaline semiterrestrial crab *Chasmagnathus granulatus*: interaction between D1- and D2-like receptors. *J Exp Biol* **209**, 2785-2793.

Halperin, J., Genovese, G., Tresguerres, M. and Luquet, C. M. (2004). Modulation of ion uptake across posterior gills of the crab *Chasmagnathus granulatus* by dopamine and cAMP. *Comp Biochem Physiol A Mol Integr Physiol* **139**, 103-109.

Hans, S., Quijada-Rodriguez, A. R., Allen, G. J. P., Onken, H., Treberg, J. R. and Weihrauch, D. (2018). Ammonia excretion and acid-base regulation in the American horseshoe crab, *Limulus polyphemus*. *J Exp Biol* **221**, jeb151894.

Henry, R. P., Lucu, C., Onken, H. and Weihrauch, D. (2012). Multiple functions of the crustacean gill: osmotic/ionic regulation, acid-base balance, ammonia excretion, and bioaccumulation of toxic metals. *Front Physiol* **3**, 431.

Hermann, A. and Erxleben, C. (2001). Nitric oxide activates voltage-dependent potassium currents of crustacean skeletal muscle. *Nitric Oxide* **5**, 361-369.

Hu, M. Y., Sung, P. H., Guh, Y. J., Lee, J. R., Hwang, P. P., Weihrauch, D. and Tseng, Y. C. (2017). Perfused gills reveal fundamental principles of pH regulation and ammonia

homeostasis in the Cephalopod *Octopus vulgaris*. *Front Physiol* **8**, 162.

Kaupp, U. B. and Seifert, R. (2002). Cyclic nucleotide-gated ion channels. *Physiol Rev* **82**, 769-824.

Kobiałka, M. and Gorczyca, W. A. (2000). Particulate guanylyl cyclases: multiple mechanisms of activation. *Acta Biochim Pol* **47**, 517-528.

Koizumi, T., Hayakawa, J. and Nikaido, H. (1990). Blood ammonia concentration in mice: normal reference values and changes during growth. *Lab Anim Sci* **40**, 308-311.

Larsen, E. H., Deaton, L. E., Onken, H., O'Donnell, M., Grosell, M., Dantzler, W. H. and Weihrauch, D. (2014). Osmoregulation and excretion. *Compr Physiol* **4**, 405-573.

Lazarenko, R. M., DelBove, C. E., Strothman, C. E. and Zhang, Q. (2017). Ammonium chloride alters neuronal excitability and synaptic vesicle release. *Sci Rep* **7**, 5061.

Le Moullac, G. and Haffner, P. (2000). Environmental factors affecting immune responses in Crustacea. *Aquaculture* **191**, 121-131.

Leone, F. A., Lucena, M. N., Garçon, D. P., Pinto, M. R. and McNamara, J. C. (2017). Gill ion transport ATPases and ammonia excretion in aquatic crustaceans. In *Acid-Base Balance and Nitrogen Excretion in Invertebrates*, pp. 61-107: Springer.

Lincoln, T. M. (1983). Effects of nitroprusside and 8-bromo-cyclic GMP on the contractile activity of the rat aorta. *J Pharmacol Exp Ther* **224**, 100-107.

Litvin, T. N., Kamenetsky, M., Zarifyan, A., Buck, J. and Levin, L. R. (2003). Kinetic properties of "soluble" adenylyl cyclase. Synergism between calcium and bicarbonate. *J Biol Chem* **278**, 15922-15926.

Llansola, M., Rodrigo, R., Monfort, P., Montoliu, C., Kosenko, E., Cauli, O., Piedrafita, B., El Mlili, N. and Felipo, V. (2007). NMDA receptors in hyperammonemia and hepatic encephalopathy. *Metab Brain Dis* **22**, 321-335.

Lu, Y., Zhang, J., Cao, J., Liu, P., Li, J. and Meng, X. (2022). Long-term ammonia toxicity in the hepatopancreas of swimming crab *Portunus trituberculatus*: cellular stress response and tissue damage. *Frontiers in Marine Science* **8**, 757602.

Luquet, C. M., Postel, U., Halperin, J., Urcola, M. R., Marques, R. and Siebers, D. (2002). Transepithelial potential differences and Na^+ flux in isolated perfused gills of the crab

Chasmagnathus granulatus (Grapsidae) acclimated to hyper- and hypo-salinity. *J Exp Biol* **205**, 71-77.

Martin, M., Fehsenfeld, S., Sourial, M. M. and Weihrauch, D. (2011). Effects of high environmental ammonia on branchial ammonia excretion rates and tissue Rh-protein mRNA expression levels in seawater acclimated Dungeness crab *Metacarcinus magister*. *Comp Biochem Physiol A Mol Integr Physiol* **160**, 267-277.

Martinelle, K. and Häggström, L. (1993). Mechanisms of ammonia and ammonium ion toxicity in animal cells: transport across cell membranes. *Journal of biotechnology* **30**, 339-350.

Matthews, J. B., Awtrey, C. S. and Madara, J. L. (1992). Microfilament-dependent activation of $Na^+/K^+/2Cl^-$ cotransport by cAMP in intestinal epithelial monolayers. *J Clin Invest* **90**, 1608-1613.

Mayer, B., Pfeiffer, S., Schrammel, A., Koesling, D., Schmidt, K. and Brunner, F. (1998). A new pathway of nitric oxide/cyclic GMP signaling involving S-nitrosoglutathione. *J Biol Chem* **273**, 3264-3270.

Meseck, S. L., Alix, J. H., Swiney, K. M., Long, W. C., Wikfors, G. H. and Foy, R. J. (2016). Ocean Acidification Affects Hemocyte Physiology in the Tanner Crab (*Chionoecetes bairdi*). *PLoS One* **11**, e0148477.

Mo, N., Shao, S., Zhuang, Y., Yang, Y., Cui, Z. and Bao, C. (2024). Activation and characterization of G protein-coupled receptors for CHHs in the mud crab, *Scylla paramamosain*. *Comp Biochem Physiol A Mol Integr Physiol* **288**, 111563.

Mohan, S., Tiwari, M. N., Biala, Y. and Yaari, Y. (2019). Regulation of neuronal Na^+/K^+-ATPase by specific protein kinases and protein phosphatases. *J Neurosci* **39**, 5440-5451.

Morris, S. and Butler, S. L. (1996). Hemolymph respiratory gas, acid-base, and ion status of the amphibious purple shore crab *Leptograpsus variegatus* (Fabricius) during immersion and environmental hypoxia. *Journal of Crustacean Biology* **16**, 253-266.

Napolitano, L. M. R., Torre, V. and Marchesi, A. (2021). CNG channel structure, function, and gating: a tale of conformational flexibility. *Pflugers Arch* **473**, 1423-1435.

Ni, Y., Wu, R., Xu, W., Maecke, H., Flammer, J. and Haefliger, I. O. (2006). Effect of

cAMP on porcine ciliary transepithelial short-circuit current, sodium transport, and chloride transport. *Invest Ophthalmol Vis Sci* **47**, 2065-2074.

O'Donnell, M. J., Dow, J. A., Huesmann, G. R., Tublitz, N. J. and Maddrell, S. H. (1996). Separate control of anion and cation transport in malpighian tubules of *Drosophila Melanogaster*. *J Exp Biol* **199**, 1163-1175.

Oliphant, A., Alexander, J. L., Swain, M. T., Webster, S. G. and Wilcockson, D. C. (2018). Transcriptomic analysis of crustacean neuropeptide signaling during the moult cycle in the green shore crab, *Carcinus maenas*. *BMC Genomics* **19**.

Onken, H. and Riestenpatt, S. (2002). Ion transport across posterior gills of hyperosmoregulating shore crabs (*Carcinus maenas*): amiloride blocks the cuticular Na^+ conductance and induces current-noise. *J Exp Biol* **205**, 523-531.

Onken, H. and Siebers, D. (1992). Voltage-clamp measurements on single split lamellae of posterior gills of the shore crab *Carcinus maenas*. *Marine Biology* **114**, 385-390.

Ostrom, K. F., LaVigne, J. E., Brust, T. F., Seifert, R., Dessauer, C. W., Watts, V. J. and Ostrom, R. S. (2022). Physiological roles of mammalian transmembrane adenylyl cyclase isoforms. *Physiol Rev* **102**, 815-857.

Pasmanter, N., Iheanacho, F. and Hashmi, M. F. (2019). Biochemistry, cyclic GMP.

Peter, M. C. S. and Gayathry, R. (2021). Nitric oxide synthase (NOS) inhibitor L-NAME activates inducible NOS/NO system and drives multidimensional regulation of Na^+/K^+-ATPase in ionocyte epithelia of immersion-stressed air-breathing fish (*Anabas testudineus Bloch*). *J Exp Zool A Ecol Integr Physiol* **335**, 396-416.

Pietrobon, M., Zamparo, I., Maritan, M., Franchi, S. A., Pozzan, T. and Lodovichi, C. (2011). Interplay among cGMP, cAMP, and Ca^{2+} in living olfactory sensory neurons *in vitro* and *in vivo*. *J Neurosci* **31**, 8395-8405.

Pitts, N. L. and Mykles, D. L. (2015). Nitric oxide production and sequestration in the sinus gland of the green shore crab *Carcinus maenas*. *J Exp Biol* **218**, 353-362.

Porro, A., Saponaro, A., Castelli, R., Introini, B., Hafez Alkotob, A., Ranjbari, G., Enke, U., Kusch, J., Benndorf, K., Santoro, B. et al. (2024). A high affinity switch for cAMP in the HCN pacemaker channels. *Nat Commun* **15**, 843.

Postel, U., Petrausch, G., Riestenpatt, S., Weihrauch, D., Malykh, J., Becker, W. and Siebers, D. (1998). Inhibition of Na^+/K^+-ATPase and of active ion-transport functions in the gills of the shore crab *Carcinus maenas* induced by cadmium. *Marine Biology* **130**, 407-416.

Poulsen, H., Morth, P., Egebjerg, J. and Nissen, P. (2010). Phosphorylation of the Na^+,K^+-ATPase and the H^+,K^+-ATPase. *FEBS Lett* **584**, 2589-2595.

Purves, G. I., Kamishima, T., Davies, L. M., Quayle, J. M. and Dart, C. (2009). Exchange protein activated by cAMP (Epac) mediates cAMP-dependent but protein kinase A-insensitive modulation of vascular ATP-sensitive potassium channels. *J Physiol* **587**, 3639-3650.

Quijada-Rodriguez, A. R., Allen, G. J. P., Nash, M. T. and Weihrauch, D. (2022). Postprandial nitrogen and acid-base regulation in the seawater acclimated green crab, *Carcinus maenas*. *Comp Biochem Physiol A Mol Integr Physiol* **267**, 111171.

Quijada-Rodriguez, A. R., Fehsenfeld, S., Marini, A. M., Wilson, J. M., Nash, M. T., Sachs, M., Towle, D. W. and Weihrauch, D. (2024). Branchial CO_2 and ammonia excretion in crustaceans: Involvement of an apical Rhesus-like glycoprotein. *Acta Physiologica* **240**, e14078.

Quijada-Rodriguez, A. R., Schultz, A. G., Wilson, J. M., He, Y., Allen, G. J. P., Goss, G. G. and Weihrauch, D. (2017). Ammonia-independent sodium uptake mediated by Na^+ channels and NHEs in the freshwater ribbon leech *Nephelopsis obscura*. *J Exp Biol* **220**, 3270-3279.

Quijada-Rodriguez, A. R., Treberg, J. R. and Weihrauch, D. (2015). Mechanism of ammonia excretion in the freshwater leech *Nephelopsis obscura*: characterization of a primitive Rh protein and effects of high environmental ammonia. *Am J Physiol Regul Integr Comp Physiol* **309**, R692-R705.

Rahman, N., Buck, J. and Levin, L. R. (2013). pH sensing *via* bicarbonate-regulated "soluble" adenylyl cyclase (sAC). *Front Physiol* **4**, 343.

Reif, D. W. and McCreedy, S. A. (1995). N-nitro-L-arginine and N-monomethyl-L-arginine exhibit a different pattern of inactivation toward the three nitric oxide synthases. *Arch Biochem Biophys* **320**, 170-176.

Ridgel, A. L., Peacock, C. A., Fickes, E. J. and Kim, C. H. (2012). Active-assisted cycling improves tremor and bradykinesia in Parkinson's disease. *Arch Phys Med Rehabil* **93**, 2049-54.

Riestenpatt, S., Onken, H. and Siebers, D. (1996). Active absorption of Na^+ and Cl^- across the gill epithelium of the shore crab *Carcinus maenas*: voltage-clamp and ion-flux studies. *J Exp Biol* **199**, 1545-1554.

Robichaux, W. G., 3rd and Cheng, X. (2018). Intracellular cAMP sensor EPAC: physiology, pathophysiology, and therapeutics development. *Physiol Rev* **98**, 919-1053.

Rybalkin, S. D., Yan, C., Bornfeldt, K. E. and Beavo, J. A. (2003). Cyclic GMP phosphodiesterases and regulation of smooth muscle function. *Circ Res* **93**, 280-291.

Schmidt, H. H., Pollock, J. S., Nakane, M., Forstermann, U. and Murad, F. (1992). Ca^{2+}/calmodulin-regulated nitric oxide synthases. *Cell Calcium* **13**, 427-434.

Schuster, D., Khanppnavar, B., Kantarci, I., Mehta, V. and Korkhov, V. M. (2024). Structural insights into membrane adenylyl cyclases, initiators of cAMP signaling. *Trends Biochem Sci* **49**, 156-168.

Seino, S. and Shibasaki, T. (2005). PKA-dependent and PKA-independent pathways for cAMP-regulated exocytosis. *Physiol Rev* **85**, 1303-1342.

Shin, K. W., Kim, S.-H., Kim, J.-H., Hwang, S. D. and Kang, J.-C. (2016). Toxic effects of ammonia exposure on growth performance, hematological parameters, and plasma components in rockfish, *Sebastes schlegelii*, during thermal stress. *Fisheries and Aquatic Sciences* **19**, 1-8.

Siebers, D., Winkler, A., Lucu, C., Thedens, G. and Weichart, D. (1985). Na-K-ATPase generates an active transport potential in the gills of the hyperregulating shore crab *Carcinus maenas*. *Marine Biology* **87**, 185-192.

Sinha, A. K., Liew, H. J., Nawata, C. M., Blust, R., Wood, C. M. and De Boeck, G. (2013). Modulation of Rh glycoproteins, ammonia excretion and Na+ fluxes in three freshwater teleosts when exposed chronically to high environmental ammonia. *J Exp Biol* **216**, 2917-2930.

Skold, H. N., Norstrom, E. and Wallin, M. (2002). Regulatory control of both microtubule- and actin-dependent fish melanosome movement. *Pigment Cell Res* **15**, 357-366.

Spaargaren, D. (1990). The effect of total environmental CO_2 concentrations on the ion-permeability of shore crabs, *Carcinus maenas* (L.). *Comparative Biochemistry and Physiology Part A: Physiology* **95**, 379-384.

Stuehr, D., Pou, S. and Rosen, G. M. (2001). Oxygen reduction by nitric-oxide synthases. *J Biol Chem* **276**, 14533-14536.

Sürmeli, N. B., Muskens, F. M. and Marletta, M. A. (2015). The influence of nitric oxide on soluble guanylate cyclase regulation by nucleotides: role of the pseudosymmetric site. *J Biol Chem* **290**, 15570-15580.

Taylor, S. S., Zhang, P., Steichen, J. M., Keshwani, M. M. and Kornev, A. P. (2013). PKA: lessons learned after twenty years. *Biochim Biophys Acta* **1834**, 1271-1278.

Thiel, D., Hugenschutt, M., Meyer, H., Paululat, A., Quijada-Rodriguez, A. R., Purschke, G. and Weihrauch, D. (2017). Ammonia excretion in the marine polychaete *Eurythoe complanata* (Annelida). *J Exp Biol* **220**, 425-436.

Towle, D. W., Henry, R. P. and Terwilliger, N. B. (2011). Microarray-detected changes in gene expression in gills of green crabs (*Carcinus maenas*) upon dilution of environmental salinity. *Comp Biochem Physiol Part D Genomics Proteomics* **6**, 115-125.

Towle, D. W., Rushton, M. E., Heidysch, D., Magnani, J. J., Rose, M. J., Amstutz, A., Jordan, M. K., Shearer, D. W. and Wu, W. S. (1997). Sodium/proton antiporter in the euryhaline crab *Carcinus maenas*: molecular cloning, expression and tissue distribution. *J Exp Biol* **200**, 1003-1014.

Towle, D. W. and Weihrauch, D. (2001). Osmoregulation by gills of euryhaline crabs: molecular analysis of transporters. *American Zoologist* **41**, 770-780.

Vielmuth, F., Radeva, M. Y., Yeruva, S., Sigmund, A. M. and Waschke, J. (2023). cAMP: A master regulator of cadherin-mediated binding in endothelium, epithelium and myocardium. *Acta Physiologica* **238**, e14006.

Voss, M., Vitavska, O., Walz, B., Wieczorek, H. and Baumann, O. (2007). Stimulus-induced phosphorylation of vacuolar H^+-ATPase by protein kinase A. *J Biol Chem* **282**, 33735-33742.

Wall, M. E., Francis, S. H., Corbin, J. D., Grimes, K., Richie-Jannetta, R., Kotera, J.,

Macdonald, B. A., Gibson, R. R. and Trewhella, J. (2003). Mechanisms associated with cGMP binding and activation of cGMP-dependent protein kinase. *Proc Natl Acad Sci U S A* **100**, 2380-2385.

Wall, S. M. (1996). Ammonium transport and the role of the Na,K-ATPase. *Miner Electrolyte Metab* **22**, 311-317.

Weihrauch, D. (1995). Zur Stickstoff-Exkretion der Strandkrabbe *Carcinus maenas*/vorgelegt von Dirk Weihrauch.

Weihrauch, D. (2006). Active ammonia absorption in the midgut of the Tobacco hornworm *Manduca sexta* L.: transport studies and mRNA expression analysis of a Rhesus-like ammonia transporter. *Insect Biochem Mol Biol* **36**, 808-821.

Weihrauch, D. and Allen, G. J. P. (2018). Ammonia excretion in aquatic invertebrates: new insights and questions. *J Exp Biol* **221**, jeb169219.

Weihrauch, D., Becker, W., Postel, U., Luck-Kopp, S. and Siebers, D. (1999). Potential of active excretion of ammonia in three different haline species of crabs. *Journal of Comparative Physiology B* **169**, 25-37.

Weihrauch, D., Becker, W., Postel, U., Riestenpatt, S. and Siebers, D. (1998). Active excretion of ammonia across the gills of the shore crab *Carcinus maenas* and its relation to osmoregulatory ion uptake. *Journal of Comparative Physiology B* **168**, 364-376.

Weihrauch, D., Chan, A. C., Meyer, H., Doring, C., Sourial, M. and O'Donnell, M. J. (2012). Ammonia excretion in the freshwater planarian *Schmidtea mediterranea*. *J Exp Biol* **215**, 3242-3253.

Weihrauch, D., Fehsenfeld, S. and Quijada-Rodriguez, A. (2017). Nitrogen excretion in aquatic crustaceans. In *Acid-Base Balance and Nitrogen Excretion in Invertebrates*, pp. 1-24: Springer.

Weihrauch, D. and McGaw, I. (2023). Ecophysiology of the European Green Crab (*Carcinus Maenas*) and Related Species: Mechanisms Behind the Success of a Global Invader: Elsevier.

Weihrauch, D., McNamara, J. C., Towle, D. W. and Onken, H. (2004a). Ion-motive ATPases and active, transbranchial NaCl uptake in the red freshwater crab, *Dilocarcinus pagei*

(Decapoda, Trichodactylidae). *J Exp Biol* **207**, 4623-4631.

Weihrauch, D., Morris, S. and Towle, D. W. (2004b). Ammonia excretion in aquatic and terrestrial crabs. *J Exp Biol* **207**, 4491-4504.

Weihrauch, D. and O'Donnell, M. (2017). Acid-Base Balance and Nitrogen Excretion in Invertebrates: Springer.

Weihrauch, D., Wilkie, M. P. and Walsh, P. J. (2009). Ammonia and urea transporters in gills of fish and aquatic crustaceans. *J Exp Biol* **212**, 1716-1730.

Weihrauch, D., Ziegler, A., Siebers, D. and Towle, D. W. (2001). Molecular characterization of V-type H^+-ATPase (B-subunit) in gills of euryhaline crabs and its physiological role in osmoregulatory ion uptake. *J Exp Biol* **204**, 25-37.

Weihrauch, D., Ziegler, A., Siebers, D. and Towle, D. W. (2002). Active ammonia excretion across the gills of the green shore crab *Carcinus maenas*: participation of Na^+/K^+-ATPase, V-type H^+-ATPase and functional microtubules. *J Exp Biol* **205**, 2765-2775.

Worrell, R. T., Merk, L. and Matthews, J. B. (2008). Ammonium transport in the colonic crypt cell line, T84: role for Rhesus glycoproteins and NKCC1. *Am J Physiol Gastrointest Liver Physiol* **294**, G429-G440.

Wright, P. A. (1995). Nitrogen excretion: three end products, many physiological roles. *J Exp Biol* **198**, 273-281.

Wright, P. A., Part, P. and Wood, C. M. (1995). Ammonia and urea excretion in the tidepool sculpin (*Oligocottus maculosus*): sites of excretion, effects of reduced salinity and mechanisms of urea transport. *Fish Physiol Biochem* **14**, 111-123.

Wright, P. A. and Wood, C. M. (2012). Seven things fish know about ammonia and we don't. *Respir Physiol Neurobiol* **184**, 231-240.

Xu, Z., Wei, Y., Huang, H., Guo, S. and Ye, H. (2022). Immunomodulatory role of short neuropeptide F in the mud crab *Scylla paramamosain*. *Dev Comp Immunol* **126**, 104260.

Zaccolo, M. and Movsesian, M. A. (2007). cAMP and cGMP signaling cross-talk: role of phosphodiesterases and implications for cardiac pathophysiology. *Circ Res* **100**, 1569-1578.

Zhang, X., Pan, L., Wei, C., Tong, R., Li, Y., Ding, M. and Wang, H. (2020). Crustacean hyperglycemic hormone (CHH) regulates the ammonia excretion and metabolism in white

shrimp, *Litopenaeus vannamei* under ammonia-N stress. *Sci Total Environ* **723**, 138128.

Zhouyao, H., Zimmer, A. M., Fehsenfeld, S., Liebenstein, T., Richter, D. O., Begemann, G., Eck, P., Perry, S. F. and Weihrauch, D. (2022). Characterization of two novel ammonia transporters, Hiat1a and Hiat1b, in the teleost model system *Danio rerio*. *J Exp Biol* **225**, jeb244279.